

Federated Learning over Noisy Channels: Convergence Analysis and Design Examples

Xizixiang Wei Cong Shen

Abstract

Does Federated Learning (FL) work when *both* uplink and downlink communications have errors? How much communication noise can FL handle and what is its impact to the learning performance? This work is devoted to answering these practically important questions by explicitly incorporating both uplink and downlink noisy channels in the FL pipeline. We present several novel convergence analyses of FL over simultaneous uplink and downlink noisy communication channels, which encompass full and partial clients participation, direct model and model differential transmissions, and non-independent and identically distributed (IID) local datasets. These analyses characterize the sufficient conditions for FL over noisy channels to have the same convergence behavior as the ideal case of no communication error. More specifically, in order to maintain the $\mathcal{O}(1/T)$ convergence rate of FEDAVG with perfect communications, the uplink and downlink signal-to-noise ratio (SNR) for direct model transmissions should be controlled such that they scale as $\mathcal{O}(t^2)$ where t is the index of communication rounds, but can stay constant for model differential transmissions. The key insight of these theoretical results is a “flying under the radar” principle – stochastic gradient descent (SGD) is an inherent noisy process and uplink/downlink communication noises can be tolerated as long as they do not dominate the time-varying SGD noise. We exemplify these theoretical findings with two widely adopted communication techniques – transmit power control and diversity combining – and further validating their performance advantages over the standard methods via extensive numerical experiments using several real-world FL tasks.

I. INTRODUCTION

Federated learning (FL) [1], [2] is an emerging distributed machine learning paradigm that has many attractive properties which can address new challenges in machine learning (ML). In particular, FL is motivated by the growing trend that massive amount of the real-world data are *exogenously* generated at

The authors are with the Charles L. Brown Department of Electrical and Computer Engineering, University of Virginia, Charlottesville, VA 22904, USA. E-mail: {xw8cw, cong}@virginia.edu.

The work was partially supported by the US National Science Foundation (NSF) under Grant ECCS-2033671.

the edge devices. For better privacy protection, it is desirable to keep the data locally at the device and enable distributed model training, which has motivated the development of FL. The power of FL has been realized in commercial devices (e.g., Google Pixel 2 uses FL to train ML models to personalize user experience) and ML tasks (e.g., Gboard uses FL for keyboard prediction) [3].

Communication efficiency has been at the front and center of FL ever since its inception [1], [2], and it is widely regarded as one of its primary bottlenecks [4], [5]. Early research has largely focused on either reducing the number of communication rounds [1], [6], or decreasing the size of the payload for transmission [5], [7]–[9]. This is because in most FL literature that deals with communication efficiency, it is often assumed that a perfect communication “tunnel” has been established, and the task of improving communication efficiency largely resides on the ML design that trades off computation and communication. More recent research starts to fill this gap by focusing on the communication system design, particularly for wireless FL [10], [11] where the underlying communication is unreliable; see Section II for an overview. Nevertheless, the focus has been on resource allocation [12]–[14], device selection [15]–[18], or either uplink or downlink (but not both) cellular system design [13], [19].

While the early studies provide a glimpse of the potential of optimizing the communication design for FL, the important issue of *noisy communications for both uplink* (clients send local models to the parameter server) *and downlink* (server sends global model to clients) have not been well investigated. In particular, it is often taken for granted that standard communication techniques can be directly applied to FL. We show in this paper that this can be highly suboptimal because they are mostly designed for independent and identically distributed (IID) sources (over time), while the communicated local and global models in both communication directions of FL represent a long-term process consisting of many progressive rounds of model updating that collectively determine the final learning outcome. Channel noise or bit/packet error rates cannot be directly translated to the ultimate ML model accuracy and convergence rate. It is thus important to rethink the communication designs in both uplink and downlink that cater to the unique characteristics of FL.

The goal of this paper is to answer the following questions: how much communication noise can FL handle, and what is its impact to the learning performance? Towards this end, we first describe a complete FL system where both model upload and download take place over noisy channels. We then present the first major contribution of this work – novel convergence analyses of the standard FEDAVG scheme under non-IID datasets, full or partial clients participation, direct model or model differential transmissions, and noisy downlink and uplink channels. These analyses are based on very general noise assumptions, and hence are broadly applicable to a variety of practical communication systems. More importantly, the analyses reveal that, in order to maintain the same $\mathcal{O}(1/T)$ convergence rate of FEDAVG with perfect

communications (the ideal case), the uplink and downlink signal-to-noise-ratio (SNR) should be controlled such that they scale as $\mathcal{O}(t^2)$ where t is the index of communication rounds, when the updated local or global model is directly transmitted over the noisy channel. Furthermore, this holds for both full and partial clients participation, the latter of which is significantly more difficult to analyze. On the other hand, when only model differential is transmitted on the uplink, we show that a *constant* SNR is sufficient to achieve the $\mathcal{O}(1/T)$ convergence rate, despite the fact that both uplink and downlink noise instances exist in the aggregated global model. The key insight of these theoretical results is a “flying under the radar” principle: stochastic gradient descent (SGD) is inherently a noisy process, and as long as uplink/downlink channel noises do not dominate the SGD noise during model training, which is controlled by the time-varying learning rate, the convergence behavior is not affected. This general principle is exemplified with two widely adopted communication techniques – transmit power control and diversity combining – by controlling the resulting SNR to satisfy the theoretical analyses. Comprehensive numerical evaluations on three widely adopted ML tasks with increasing difficulties, *MNIST*, *CIFAR-10* and *Shakespeare*, are carried out using these techniques. We design a series of experiments to demonstrate that the fine-tuned transmit power control and diversity combining that are guided by the theoretical analyses can significantly outperform the equal-SNR-over-time baseline, and in fact can approach the ideal noise-free communication performance in many of the experiment settings. These results not only corroborate the theoretical conclusions but also highlight the benefit of designing communication algorithms that are specifically tailored to the characteristics of FL.

The remainder of this paper is organized as follows. Related works are surveyed in Section II. The system model that captures the noisy channels in both uplink and downlink of FL is described in Section III. Theoretical analyses are presented in Section IV for three different FL configurations. These results inspire novel communication designs, for which two examples of transmit power control and diversity combining are presented in Section V. Experimental results are given in Section VI, followed by the conclusions in Section VII. All technical proofs are given in the Appendices.

II. RELATED WORKS

Federated Learning [1] focuses on many clients collaboratively training a ML model under the coordination of a central server while keeping the local training data private at each user. It has been extensively studied in recent years in the machine learning and artificial intelligence community, which aims to address various questions around improving machine learning efficiency and effectiveness [20]–[23], preserving the privacy of user data [24], [25], robustness to attacks and failures [26], and ensuring fairness and addressing sources of bias [3], [27].

Among the various challenges associated with FL, improving the communication efficiency has attracted a lot of interest [4], [5]. One of the representative approaches for reducing the communication rounds is FEDAVG [1], which allows periodic model aggregation and local model updates and thus enables flexible communication-computation tradeoff [6]. Theoretical understanding of this tradeoff has been actively pursued and, depending on the underlying assumptions (e.g., IID or non-IID local datasets, convex or non-convex loss functions, gradient descent or stochastic gradient descent), rigorous analysis of the convergence behavior has been carried out [20], [21], [23], [28]. For the approach of reducing the size of the exchanged messages in each round, general discussions on sparsification, subsampling, and quantization are given in [2]. There have been recent efforts in developing quantization and source coding to reduce the communication cost [7]–[9], [19], [29]–[31]. Nevertheless, they mostly focus on either uplink or downlink but not both, and largely consider only full clients participation.

Recent years have also seen increased effort in the communication algorithm, protocol, and system design of FL. The inherent trade-off between local model update and global model aggregation is studied in [32] to optimize over transmission power/rate and training time. Various radio resource allocation and client selection policies [12], [16]–[18], [33]–[35] have been proposed to minimize the learning loss or the training time. Joint communication and computation is investigated [13], [15], [30], [36], [37]. In particular, the analog aggregation design [13], [30], [37], [38] serves as one of our design examples in Section V. The effect of noise has been studied in [39], [40], but the emphasis has been on how to modify the machine learning methods to reduce noise, while our work keeps the model training aspect of FL unchanged and focuses on the communication design that controls the effective noise.

III. SYSTEM MODEL

We first introduce the standard FL problem formulation, and then describe a complete FL pipeline where both local model upload and global model download take place over noisy channels.

A. FL Problem Formulation

The general federated learning problem setting studied in this paper mostly follows the standard model in the original paper [1]. In particular, we consider a FL system with one central parameter server (e.g., base station) and a set of at most N clients (e.g., mobile devices). Client $n \in [N] \triangleq \{1, 2, \dots, N\}$ stores a local dataset $\mathcal{D}_n = \{\mathbf{z}_i\}_{i=1}^{D_n}$, with its size denoted by D_n , that never leaves the client. Datasets across clients are assumed to be non-IID and disjoint. The maximum data size when all clients participate in FL is $D = \sum_{n=1}^N D_n$. The loss function $f(\mathbf{w}, \mathbf{z})$ measures how well a ML model with parameter $\mathbf{w} \in \mathbb{R}^d$

fits a single data sample \mathbf{z} . Without loss of generality, we assume that \mathbf{w} has zero-mean and unit-variance elements¹, i.e., $\mathbb{E}[|w_i|^2] = 1, \forall i \in [d]$. For the n -th client, its local loss function $F_n(\cdot)$ is defined by

$$F_n(\mathbf{w}) \triangleq \frac{1}{D_n} \sum_{\mathbf{z} \in \mathcal{D}_n} f(\mathbf{w}, \mathbf{z}).$$

The goal of FL is for the parameter server to learn a global machine learning (ML) model based on the distributed local datasets at the N clients, by coordinating and aggregating the training processes at individual clients without accessing the raw data. Specifically, the global optimization objective over all N clients is given by

$$F(\mathbf{w}) \triangleq \sum_{n=1}^N \frac{D_n}{D} F_n(\mathbf{w}) = \frac{1}{D} \sum_{n=1}^N \sum_{\mathbf{z} \in \mathcal{D}_n} f(\mathbf{w}, \mathbf{z}). \quad (1)$$

The global loss function measures how well the model fits the entire corpus of data on average. The learning objective is to find the best model parameter \mathbf{w}^* that minimizes the global loss function: $\mathbf{w}^* = \arg \min_{\mathbf{w}} F(\mathbf{w})$. Let F^* and F_k^* be the minimum value of F and F_k , respectively. Then, $\Gamma = F^* - \frac{1}{N} \sum_{k=1}^N F_k^*$ quantifies the degree of non-IID as shown in [23].

B. FL over Noisy Uplink and Downlink Channels

We study a generic FL framework where *partial* client participation and *non-IID* local datasets, two critical features that separate FL from conventional distributed ML, are explicitly captured. Unlike the existing literature, we focus on imperfect communications and consider that *both* the upload and download transmissions take place over noisy communication channels. The overall system diagram is depicted in Fig. 1. In particular, the FL-over-noisy-channel pipeline works by iteratively executing the following steps at the t -th learning round, $\forall t \in [T]$.

(1) Downlink communication for global model download. The centralized server broadcasts the current global ML model, which is described by the latest weight vector \mathbf{w}_{t-1} from the previous round, to a set of uniformly randomly selected clients² denoted as \mathcal{S}_t with $|\mathcal{S}_t| = K$. Because of the imperfection introduced in communications, client k receives a noisy version of \mathbf{w}_{t-1} , which is written as

$$\hat{\mathbf{w}}_{t-1}^k = \mathbf{w}_{t-1} + \mathbf{e}_t^k, \quad (2)$$

¹The parameter normalization and de-normalization method can be found in the appendix in [13].

²We note that for partial clients participation, we have $K < N$; in the case of full clients participation we have $K = N$.

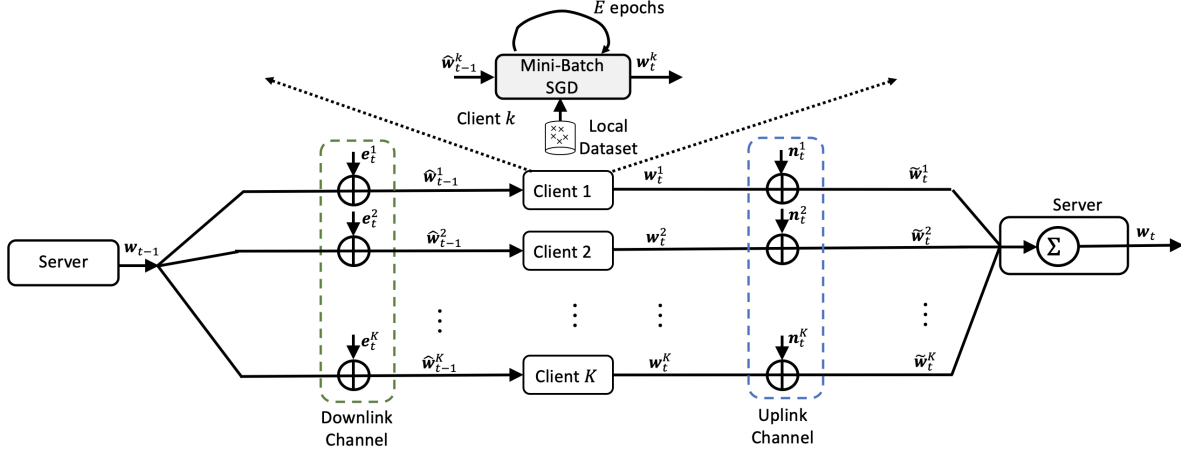


Fig. 1. End-to-end FL system diagram in the t th communication round. The impact of noisy channels in both uplink and downlink is captured.

where $\mathbf{e}_t^k = [e_{t,1}^k, \dots, e_{t,d}^k]^T \in \mathbb{R}^d$ is the d -dimensional downlink *effective noise* vector at client k and time t . We assume that \mathbf{e}_t^k is a zero-mean random vector consisting of IID elements with variance:

$$\mathbb{E}||e_{t,i}^k||^2 = \zeta_{t,k}^2 \quad \text{and} \quad \mathbb{E}||\mathbf{e}_t^k||^2 = d\zeta_{t,k}^2, \quad \forall t \in [T], k \in \mathcal{S}_t, i \in [d]. \quad (3)$$

Note that the effective noise term does not necessarily correspond to only the channel noise; it also captures post-processing errors in a communication transceiver, such as estimation, decoding and demodulation, frequency offset and phase noise, etc. We further note that the noise assumption is very mild – Eqn. (3) only requires a bounded variance of the random noise, but does not limit to any particular distribution. We define the local (post-processing) receive SNR for the k -th client at the t -th communication round as

$$\text{SNR}_{t,k}^L = \frac{\mathbb{E}||\mathbf{w}_{t-1}||^2}{\mathbb{E}||\mathbf{e}_t^k||^2} = \frac{1}{\zeta_{t,k}^2},$$

where we assume without loss of generality that the transmit power of each scalar model parameter is normalized: $\mathbb{E}||w_{t-1,i}||^2 = 1, \forall i \in [d]$. Note that this corresponds to the normalized weight described in Section III-A. In addition, we remark that the downlink communication model is very general in the sense that the effective noise variances, $\{\zeta_{t,k}^2\}$, can be different for different clients and at different rounds.

(2) Local computation. Each client uses its local data to train a local ML model improved upon the received global ML model. In this work, we assume that mini-batch stochastic gradient descent (SGD) is used in the model training. Note that this is the most commonly adopted training method in modern ML tasks, e.g., deep neural networks, but its analysis is much more complicated than gradient descent (GD) when communication noise is present.

Specifically, mini-batch SGD operates by updating the weight iteratively (for E steps in each learning round) at client k as follows:

$$\begin{aligned} \text{Initialization:} \quad & \mathbf{w}_{t,0}^k = \hat{\mathbf{w}}_{t-1}^k, \\ \text{Iteration:} \quad & \mathbf{w}_{t,\tau}^k = \mathbf{w}_{t,\tau-1}^k - \eta_t \nabla F_k(\mathbf{w}_{t,\tau-1}^k, \xi_\tau^k), \forall \tau = 1, \dots, E, \\ \text{Output:} \quad & \mathbf{w}_t^k = \mathbf{w}_{t,E}^k, \end{aligned}$$

where ξ_τ^k is a batch of data points that are sampled independently and uniformly at random from the local dataset of client k in the τ -th iteration of mini-batch SGD.

(3) Uplink communication for local model upload. The K participating clients upload their latest local models to the server. More specifically, client k transmits a vector \mathbf{x}_t^k to the server at the t -th round. We again consider the practical case where the upload communication is erroneous, and the server receives a noisy version of the individual weight vectors from each client due to various imperfections in the uplink communications (e.g. channel noise, transmitter and receiver distortion, processing error). The received vector for client k can be written as

$$\hat{\mathbf{x}}_t^k = \mathbf{x}_t^k + \mathbf{n}_t^k, \quad (4)$$

where $\mathbf{n}_t^k \in \mathbb{R}^d$ is the d -dimensional effective uplink noise vector for decoding client k 's model at time t . We assume that \mathbf{n}_t^k is a zero-mean random vector consisting of IID elements with bounded variance:

$$\mathbb{E} \|n_{t,i}^k\|^2 = \sigma_{t,k}^2 \quad \text{and} \quad \mathbb{E} \|\mathbf{n}_t^k\|^2 = d\sigma_{t,k}^2, \quad \forall t \in [T], k \in \mathcal{S}_t, i \in [d]. \quad (5)$$

We again note that the uplink communication model in Eqn. (5) is very general in the sense that (1) only bounded variance is assumed as opposed to the specific noise distribution; and (2) the effective noise variances, $\{\sigma_{t,k}^2\}$, can be different for different clients and at different rounds.

Two different choices of the vector \mathbf{x}_t^k for model upload are considered in this paper.

1) **Model Transmission (MT).** The K participating clients upload the latest local models \mathbf{w}_t^k :

$$\mathbf{x}_t^k = \mathbf{w}_t^k.$$

Following (4), the server receives the updated local model of client k as

$$\tilde{\mathbf{w}}_t^k = \hat{\mathbf{x}}_t^k = \mathbf{w}_t^k + \mathbf{n}_t^k. \quad (6)$$

2) **Model Differential Transmission (MDT).** The K participating clients only upload the differences

between the latest local model and the previously received (noisy) global model, i.e.,

$$\mathbf{x}_t^k = \mathbf{d}_t^k \triangleq \mathbf{w}_t^k - \hat{\mathbf{w}}_{t-1}^k.$$

For MDT, the server uses \mathbf{d}_t^k and the previously computed global model \mathbf{w}_{t-1} to reconstruct the updated local model of client k as

$$\tilde{\mathbf{w}}_t^k = \mathbf{w}_{t-1} + \hat{\mathbf{x}}_t^k = \mathbf{w}_{t-1} + \mathbf{d}_t^k + \mathbf{n}_t^k = \mathbf{w}_t^k + \mathbf{n}_t^k - \mathbf{e}_t^k. \quad (7)$$

The SNR for these two models, however, has to be defined slightly differently because we have normalized the ML model parameter \mathbf{w} to have unit-variance elements in Section III-A. Thus, for MT, we can write the receive SNR at the server for k -th client's signal as

$$\text{SNR}_{t,k}^{\text{S,MT}} = \frac{\mathbb{E} \|\mathbf{w}_t^k\|^2}{\mathbb{E} \|\mathbf{n}_t^k\|^2} = \frac{1}{\sigma_{t,k}^2}. \quad (8)$$

For MDT, we keep the SNR expression general since the variance of model difference \mathbf{d}_t^k is unknown *a priori* and also changes over time. We have:

$$\text{SNR}_{t,k}^{\text{S,MDT}} = \frac{\mathbb{E} \|\mathbf{d}_t^k\|^2}{\mathbb{E} \|\mathbf{n}_t^k\|^2} = \frac{\mathbb{E} \|\mathbf{d}_t^k\|^2}{d\sigma_{t,k}^2}. \quad (9)$$

Remark 1. Both schemes can be useful in practice, depending on the specific requirements of the FL system. For example, transmitting weight differential relies on the server keeping the previous global model \mathbf{w}_{t-1} , so that the new local models can be reconstructed. This however may not always be true if the server deletes intermediate model aggregation for privacy preservation [3], which makes reconstruction from the model differential infeasible.

Remark 2. It is worth noting that the different choices of *what* to transmit are not considered in most of the existing literature because, without considering the communication error, there is no difference between them from a pure learning perspective – as long as the server can reconstruct \mathbf{w}_t^k , this aspect does not impact the learning performance [1]. However, as we see shortly, the choice becomes significant when communication errors are present.

Remark 3. Both uplink and downlink channel noises collectively impact the received local models at the server. This may be more obvious for MDT than MT (Eqn. (7) explicitly involves both noise terms). However, we note that the latest local model is trained using the previously received global model, which contains the downlink noise. As a result, both MT and MDT will be impacted by both uplink and

downlink channel noises.

(4) Global aggregation. The server aggregates the received local models to generate a new global ML model, following the standard FEDAVG [1]:

$$\mathbf{w}_t = \sum_{k \in \mathcal{S}_t} \frac{D_k}{\sum_{i \in \mathcal{S}_t} D_i} \tilde{\mathbf{w}}_t^k.$$

The server then moves on to the $(t + 1)$ -th round. For ease of exposition and to simplify the analysis, we assume in the remainder of the paper that the local dataset sizes at all clients are the same³: $D_i = D_j$, $\forall i, j \in [N]$, which leads to the following simplifications.

1) **MT.** The aggregation can be simplified as

$$\mathbf{w}_t = \frac{1}{K} \sum_{k \in \mathcal{S}_t} \tilde{\mathbf{w}}_t^k = \frac{1}{K} \sum_{k \in \mathcal{S}_t} \hat{\mathbf{x}}_t^k = \frac{1}{K} \sum_{k \in \mathcal{S}_t} (\mathbf{w}_t^k + \mathbf{n}_t^k). \quad (10)$$

2) **MDT.** The aggregation can be written as

$$\mathbf{w}_t = \frac{1}{K} \sum_{k \in \mathcal{S}_t} \tilde{\mathbf{w}}_t^k = \mathbf{w}_{t-1} + \frac{1}{K} \sum_{k \in \mathcal{S}_t} \hat{\mathbf{x}}_t^k = \frac{1}{K} \sum_{k \in \mathcal{S}_t} (\mathbf{w}_t^k + \mathbf{n}_t^k - \mathbf{e}_t^k). \quad (11)$$

For the case of MT, the SNR for the global model (after aggregation) can be written as

$$\text{SNR}_t^G = \frac{\mathbb{E} \|\sum_{k \in \mathcal{S}_t} \mathbf{w}_t^k\|^2}{\mathbb{E} \|\sum_{k \in \mathcal{S}_t} \mathbf{n}_t^k\|^2} = \frac{\mathbb{E} \|\sum_{k \in \mathcal{S}_t} \mathbf{w}_t^k\|^2}{d\sigma_t^2}, \quad (12)$$

and for MDT, the SNR for the global model can be written as

$$\text{SNR}_t^G = \frac{\mathbb{E} \|\sum_{k \in \mathcal{S}_t} \mathbf{w}_t^k\|^2}{\mathbb{E} \|\sum_{k \in \mathcal{S}_t} (\mathbf{n}_t^k - \mathbf{e}_t^k)\|^2} = \frac{\mathbb{E} \|\sum_{k \in \mathcal{S}_t} \mathbf{w}_t^k\|^2}{d(\sigma_t^2 + \zeta_t^2)}, \quad (13)$$

where $\sigma_t^2 \triangleq \sum_{k \in \mathcal{S}_t} \sigma_{t,k}^2$ and $\zeta_t^2 \triangleq \sum_{k \in \mathcal{S}_t} \zeta_{t,k}^2$ denote the total uplink and downlink effective noise power for participating clients, respectively.

Remark 4. We note that the total signal power (numerators in Eqns. (12) and (13)) is difficult to evaluate. In general, $\{\mathbf{w}_t^k\}$ are correlated across clients because the local model updates all start from (roughly) the same global model. Intuitively, once FL converges, these models will largely be the same, leading to a signal power term of dK^2 for the numerator. On the other hand, if we assume that these local models are independent across clients, which is reasonable in the early phases of FL with large local epochs, where the (roughly) same starting point has diminishing impact due to the long training period and non-IID nature of the data distribution, we can have a signal power term of dK . Nevertheless, since

³We emphasize that all the results of this paper can be extended to handle different local dataset sizes.

the SNR control can be realized by adjusting the effective noise power levels, we focus on the impact of σ_t^2 and ζ_t^2 on the FL performance in Section IV.

IV. CONVERGENCE ANALYSIS OF FL OVER NOISY CHANNELS

A. Convergence Analysis for Model Transmission for Full Clients Participation

We first analyze the convergence of FEDAVG in the presence of both uplink and downlink communication noise when direct model transmission (MT) is adopted for local model upload: $\mathbf{x}_t^k = \mathbf{w}_t^k$. To simplify the analysis and highlight the key techniques in deriving the convergence rate, we assume $K = N$ in this subsection (i.e., *full* clients participation with $\mathcal{S}_t = [K] = [N]$), and leave the case of partial clients participation to Section IV-B.

We make the following standard assumptions that are commonly adopted in the convergence analysis of FEDAVG and its variants; see [7], [8], [20], [22], [23], [41]. In particular, Assumption 1-2) indicates that we focus on strongly convex $F_k(\cdot)$, which represents a category of loss functions that are widely studied in the literature.

- Assumption 1.** 1) *L-smooth*: $\forall \mathbf{v}$ and \mathbf{w} , $F_k(\mathbf{v}) \leq F_k(\mathbf{w}) + (\mathbf{v} - \mathbf{w})^T \nabla F_k(\mathbf{w}) + \frac{L}{2} \|\mathbf{v} - \mathbf{w}\|^2$.
 2) *μ -strongly convex*: $\forall \mathbf{v}$ and \mathbf{w} , $F_k(\mathbf{v}) \geq F_k(\mathbf{w}) + (\mathbf{v} - \mathbf{w})^T \nabla F_k(\mathbf{w}) + \frac{\mu}{2} \|\mathbf{v} - \mathbf{w}\|^2$.
 3) *Bounded variance for unbiased mini-batch SGD*: The mini-batch SGD is unbiased: $\mathbb{E}[\nabla F_k(\mathbf{w}, \xi)] = \nabla F_k(\mathbf{w})$, and the variance of stochastic gradients is bounded: $\mathbb{E} \|\nabla F_k(\mathbf{w}, \xi) - \nabla F_k(\mathbf{w})\|^2 \leq \delta_k^2$, for mini-batch data ξ at client $k \in [N]$.
 4) *Uniformly bounded gradient*: $\mathbb{E} \|\nabla F_k(\mathbf{w}, \xi)\|^2 \leq H^2$ for mini-batch data ξ at client $k \in [N]$.

We present the main convergence result of MT with full clients participation in Theorem 1, whose proof can be found in Appendix A.

Theorem 1. Define $\kappa = \frac{L}{\mu}$, $\gamma = \max\{8\kappa, E\}$. Set learning rate as $\eta_t = \frac{2}{\mu(\gamma+t)}$ and adopt a SNR control policy that scales the effective uplink and downlink noise power over t such that:

$$\sigma_t^2 \leq \frac{4N^2}{\mu^2(\gamma+t-1)^2} \sim \mathcal{O}\left(\frac{1}{t^2}\right) \quad (14)$$

$$\zeta_t^2 \leq \frac{4N^2}{\mu^2(\gamma+t)(\gamma+t-2)} \sim \mathcal{O}\left(\frac{1}{t^2}\right). \quad (15)$$

where $\sigma_t^2 \triangleq \sum_{k \in [N]} \sigma_{t,k}^2$ and $\zeta_t^2 \triangleq \sum_{k \in [N]} \zeta_{t,k}^2$ denote the total uplink and downlink effective noise power, respectively. Then, under Assumption 1, the convergence of FEDAVG with non-IID datasets and

full clients participation satisfies

$$\mathbb{E} \|\mathbf{w}_T - \mathbf{w}^*\|^2 \leq \frac{1}{\gamma + T} \left[\frac{4D}{\mu^2} + (8\kappa + E) \|\mathbf{w}_0 - \mathbf{w}^*\|^2 \right] \quad (16)$$

with

$$D = \sum_{k=1}^N \frac{\delta_k^2}{N^2} + 6L\Gamma + 8(E-1)^2 H^2 + 2d.$$

Theorem 1 guarantees that even under simultaneous uplink and downlink noisy communications, the same $\mathcal{O}(1/T)$ convergence rate of FEDAVG with perfect communications can be achieved if we control the effective noise power of both uplink and downlink to scale at rate $\mathcal{O}(1/t^2)$ and choose the learning rate at $\mathcal{O}(1/t)$ over t . We note that the choice of η_t to scale as $\mathcal{O}(1/t)$ is well-known in distributed and federated learning [20]–[23], [41]–[43], which essentially controls the “noise” that is inherent to the stochastic process in SGD to gradually shrink as the FL process converges. The fundamental idea that leads to Theorem 1 is to *control the “effective channel noise” to not dominate the “effective SGD noise”*, i.e., to always have the effective channel noise floor to be below that of the SGD noise. This is reflected by the effective noise power requirement in Eqns. (14) and (15).

We further note that although the requirement of Theorem 1 is presented in terms of the effective noise power, what ultimately matters is the signal-to-noise ratio defined in Section III-B. There exist signal processing and communication techniques that can satisfy the requirement by either increasing the signal power (e.g., transmit power control) or reducing the post-processing noise power (e.g., diversity combining). We discuss design examples that realize the requirement of Theorem 1 in Section V.

B. Convergence Analysis for Model Transmission for Partial Clients Participation

We now generalize the convergence analysis for full clients participation to *partial* clients participation, where we have a given $K < N$ and uniformly randomly select a set of clients \mathcal{S}_t at round t to carry out the FL process. In this section, we mostly follow the FL system model described in Section III-B, with the only simplification that we consider *homogeneous* noise power levels at the uplink and downlink, i.e., we assume

$$\sigma_{t,k}^2 = \bar{\sigma}_t^2, \quad \text{and} \quad \zeta_{t,k}^2 = \bar{\zeta}_t^2, \quad \forall t \in [T], k \in [N]. \quad (17)$$

The main reason to introduce this simplification is due to the time-varying randomly participating clients: since \mathcal{S}_t changes over t , the total power levels also vary over t if we insist on heterogeneous noise power for different clients. Furthermore, since clients are randomly selected, the total power level becomes a random variable as well, which significantly complicates the convergence analysis. Making

this assumption would allow us to focus on the challenge with respect to the model update from partial clients participation.

Theorem 2. *Let κ , γ and η_t be the same as in Theorem 1. Adopt a SNR control policy that scales the effective uplink and downlink noise power over t such that:*

$$\bar{\sigma}_t^2 \leq \frac{4K}{\mu^2(\gamma+t-1)^2} \sim \mathcal{O}\left(\frac{1}{t^2}\right) \quad (18)$$

$$\bar{\zeta}_t^2 \leq \frac{4N}{\mu^2(\gamma+t)(\gamma+t-2)} \sim \mathcal{O}\left(\frac{1}{t^2}\right). \quad (19)$$

where $\bar{\sigma}_t^2$ and $\bar{\zeta}_t^2$ represent the individual client effective noise in the uplink and downlink, respectively, which are defined in Eqn. (17). Then, under Assumption 1, the convergence of FEDAVG with non-IID datasets and partial clients participation has the same convergence rate expression as Eqn. (16), with D being replaced as:

$$D = \sum_{k=1}^N \frac{\delta_k^2}{N^2} + 6L\Gamma + 8(E-1)^2 H^2 + \frac{N-K}{N-1} \frac{4}{K} E^2 H^2 + 2d.$$

The proof of Theorem 2 is given in Appendix B. We can see that partial clients participation does not fundamentally change the behavior of FL in the presence of uplink and downlink communication noises, and the requirement for SNR control remains largely the same.

C. Convergence Analysis for Model Differential Transmission

In this section, we consider the model differential transmission (MDT) scheme when the clients uploading model parameters. Since only model differential is transmitted, the receiver must possess a copy of the “base” model to reconstruct the updated model. This precludes using MDT in the downlink for partial clients participation, because participating clients differ from round to round, and a newly participating client does not have the “base” model of the previous round to reconstruct the new global model. We thus only focus on MDT in the uplink and MT in the downlink with partial clients participation.

Theorem 3. *Let κ , γ and η_t be the same as in Theorem 1, and the effective noise follows Eqn. (17). Adopt a SNR control policy that maintains a constant uplink SNR at each client over t :*

$$\text{SNR}_{t,k}^{S,MDT} = \nu \sim \mathcal{O}(1), \quad (20)$$

and scales the effective downlink noise power at each client over t such that:

$$\bar{\zeta}_t^2 \leq \frac{\frac{4}{\mu^2}}{\frac{1}{N}(\gamma+t)(\gamma+t-2) + \frac{1}{K}\left(1 + \frac{1}{\nu}\right)(\gamma+t)^2} \sim \mathcal{O}\left(\frac{1}{t^2}\right). \quad (21)$$

Then, under Assumption 1, the convergence of FEDAVG with non-IID datasets and partial clients participation for uplink MDT and downlink MT has the same convergence rate expression as Eqn. (16), with D being replaced as:

$$D = \sum_{k=1}^N \frac{\delta_k^2}{N^2} + 6L\Gamma + 8(E-1)^2 H^2 + \frac{N-K}{N-1} \frac{4}{K} E^2 H^2 + \frac{4E^2}{K\nu} H^2 + d.$$

The complete proof of Theorem 3 can be found in Appendix C. It is instrumental to note that unlike direct model transmission, only transmitting model differentials in the uplink allows us to remove the corresponding SNR scaling requirement. Instead, one can keep a *constant* SNR in uplink throughout the entire FL process. Intuitively, this is because the “scaling” already takes place in the model differential \mathbf{d}_t^k , which is the difference between the updated local model at client k after E epochs of training and the starting local model. As FL gradually converges, this differential becomes smaller. Thus, by keeping a constant communication SNR, we essentially scales down the effective noise power at the server.

V. COMMUNICATION DESIGN EXAMPLES FOR FL IN NOISY CHANNELS

A. Design Example 1: Transmit Power Control for Analog Aggregation

An immediate engineering question following the theoretical analysis is how we can realize the effective noise power (either $\mathcal{O}(1/t^2)$ or constant) in the theorems. One natural approach is *transmit power control*, which has the flexibility of controlling the average receive SNR (and thus the effective noise power) while satisfying the power constraint. In this work, we design a power control policy for the analog aggregation FL framework in [13], as an example to demonstrate the system design for FL tasks in the presence of communication noise.

The analog aggregation method in [13]. Consider a communication system where several narrowband orthogonal channels (e.g. sub-carriers in OFDM, time slots in TDMA, or eigenchannels in MIMO) are shared by K random selected clients in an uplink model update phase of a communication round in FEDAVG. Each element in the transmitted model $\mathbf{w} \in \mathbb{R}^d$ is allocated and transmitted in a narrowband channel and aggregated automatically over the air [13]. Denote the received signal of each element $i = 1, \dots, d$ in the t -th communication round as

$$y_{t,i} = \frac{1}{K} \sum_{k \in \mathcal{S}_t} r_{t,k}^{-\alpha/2} h_{t,k,i} p_{t,k,i} w_{t,k,i} + n_{t,i} \quad \forall k \in \mathcal{S}_t,$$

where $r_{t,k}^{-\alpha/2}$ and $h_{t,k,i} \in \mathcal{CN} \sim (0, 1)$ denote the large-scale and small-scale fading coefficients of the channel, respectively, $n_{t,i} \in \mathcal{CN} \sim (0, 1)$ is the IID additive Gaussian white noise, and $p_{t,k,i}$ denotes the transmit power determined by the power control policy. We assume perfect channel state information at

the transmitters (CSIT). Due to the aggregation requirement of federated learning, the channel inversion rule is used in [13], which leads to the following *instantaneous* transmit power of user k at time t for model weight element i :

$$p_{t,k,i} = \frac{\sqrt{\rho_t^{\text{UL}}}}{r_{t,k}^{-\alpha/2} h_{t,k,i}}, \quad (22)$$

where ρ_t is a scalar that denotes the uplink average transmit power. Hence, the received SNR of the global model can be written as

$$\text{SNR}_t^G = \mathbb{E} \left\| \sum_{i=1}^d \frac{\frac{\sqrt{\rho_t^{\text{UL}}}}{K} \sum_{k \in \mathcal{S}_t} w_{t,k,i}}{n_{t,i}} \right\|^2 = \frac{\rho_t^{\text{UL}} \mathbb{E} \left\| \sum_{k \in \mathcal{S}_t} \mathbf{w}_t^k \right\|^2}{dK^2}. \quad (23)$$

Transmit power control. The original analog aggregation framework in [13] assumes that ρ_t^{UL} is a constant over time t . However, our theoretical analysis in Section IV suggests that this can be improved. Specifically, if we take partial clients participation and MT as an example, and further assume IID weight elements, we have

$$\rho_t^{\text{UL}} = \frac{K}{\sigma_t^2} \geq \frac{\mu^2(\gamma + t - 1)^2}{4K} \sim \mathcal{O}(t^2), \quad (24)$$

by plugging in Theorem 2, which implies that ρ_t should be increased at the rate $\mathcal{O}(t^2)$ in the uplink to ensure the convergence of FEDAVG. Similar policy can be derived for MDT and/or full clients participation, by invoking the corresponding theorems.

In the downlink case, when the server broadcasts the global model to K randomly selected clients, the receive signal of the i -th element for the n -th user in the t -th communication round is

$$y_{t,n,i} = r_{t,n}^{-\alpha/2} h_{t,n,i} \sqrt{\rho_t^{\text{DL}}} w_{t,i} + e_{t,n,i} \quad \forall n = 1 \cdots K,$$

where $e_{t,n,i} \in \mathcal{CN} \sim (0, 1)$ is the IID additive Gaussian white noise, and ρ_t^{DL} is the transmitted power at the server. The downlink SNR for the n -th user is

$$\text{SNR}_{t,n,i}^L = r_{t,n}^{-\alpha} \rho_t^{\text{DL}}. \quad (25)$$

Instead of keeping ρ_t^{DL} as a constant, we derive the following policy based on Theorem 3 to guarantee the convergence of FEDAVG:

$$\rho_t^{\text{DL}} \geq \frac{r_{t,k}^\alpha \mu^2 (\gamma + t) (\gamma + t - 2)}{4N} \sim \mathcal{O}(t^2). \quad (26)$$

Finally, by applying the power control policy defined in Eqns. (24) and (26), FL tasks are able to achieve better performances under the same energy budget. This is also numerically validated in the experiment.

Remarks. We note that the proposed transmit power control only changes the *average* transmit power at learning rounds. In fact, this method can be used in conjunction with a faster power control, such as the channel inversion power in Eqn. (22) or any other methods that handle the fast fading component or interference, to determine the instantaneous transmit power of the sender. One minor note is that the pathloss component appears in Eqn. (26) but not in (24). This is due to the broadcast nature of download. For upload, the pathloss is absorbed in the channel inversion expression (22).

B. Design Example II: Receiver Diversity Combining for Analog Aggregation

Another technique that can benefit from our theoretical results is to control the diversity order of a receiver combining scheme, such as using multiple receive antennas or multiple time or frequency slots. Essentially we are leveraging the repeated transmissions to reduce the effective noise power via diversity combining, and by only activating sufficient diversity branches as we progress over the learning rounds, resources can be more efficiently utilized.

Uplink diversity requirement. We assume the updated local model is independently received P times (over time, frequency, space, or some combination of them) in the t -th communication round. Reusing the notations and the channel inversion rule in (22), the P_t received signals for the i -th element can be denoted as

$$y_{t,i,p} = \frac{1}{K} \sum_{k=1}^K \sqrt{\rho_{t,p}} w_{t,k,i} + n_{t,i,p} \quad \forall k \in \mathcal{S}_t, \quad \forall p = 1 \cdots P_t.$$

For simplicity, we write $\rho_{t,p} = \rho_0$ as the average transmit power. The received SNR of the global model after the diversity combining can be written as

$$\text{SNR}_t^G = \mathbb{E} \left\| \frac{\sum_{i=1}^d \sum_{p=1}^P \frac{\sqrt{\rho_{t,p}}}{K} \sum_{k \in \mathcal{S}_t} w_{t,k,i}}{\sum_{p=1}^P n_{t,i,p}} \right\|^2 = P_t \frac{\rho_0 \mathbb{E} \|\sum_{k \in \mathcal{S}_t} \mathbf{w}_t^k\|^2}{dK^2}.$$

Compared with the SNR of the power control policy in (23), we can derive the diversity requirement as

$$P_t = \left\lceil \frac{\rho_t^{\text{UL}}}{\rho_0} \right\rceil, \quad (27)$$

where $\lceil a \rceil$ denotes the ceiling operation on a .

Downlink diversity requirement. The server broadcasts the global weight for Q_t times (again it can be over time, frequency, space, or some combination of them) in the t -th communication round and each client combines the multiple independent copies of the received signals to achieve a higher SNR (i.e., lower effective noise power). The downlink signal can be written as

$$y_{t,k,i,q} = r_{t,n,i}^{-\alpha/2} h_{t,n,i} \sqrt{\rho_{t,q}} w_{t,i} + e_{t,k,i,q} \quad \forall n = 1 \cdots N, \quad \forall q = 1 \cdots Q_t,$$

where $\rho_{t,q} = \rho_1$ is the transmit power constraint at the server. The downlink SNR for the n -th user is

$$\text{SNR}_{t,n}^L = r_{t,n}^{-\alpha} Q_t \rho_1.$$

Similarly, compared with the local SNR in (25), we can derive the diversity requirement as

$$Q_t = \left\lceil \frac{\rho_t^{\text{DL}}}{\rho_1} \right\rceil. \quad (28)$$

By applying the combining rules in Eqns. (27) and (28), we have the complete design for receiver diversity that can guarantee the convergence of FL at rate $\mathcal{O}(1/T)$, under the transmit power constraints at both clients and server.

Remarks. Receiver diversity combining is not as flexible as power control, because it can only achieve *discrete* effective noise power levels. This is also confirmed in the experiments. However, it can be useful in situations where adjusting the average transmit power is not feasible, e.g., no change at the transmitter is allowed. In addition, one can combine the transmit power control in Section V-A with the receiver diversity combining in Section V-B in a straightforward manner. We also note that there are other methods, such as increasing the precision of Analog-to-Digital Converters (ADC), to implement the SNR control policy. The general design principles in Theorems 1 to 3 can be similarly realized.

VI. EXPERIMENT RESULTS

A. Experiment Setup

We consider a communication system with noisy uplink and downlink channels to support various FL tasks. For simplicity, we assume that every channel use has the same noise level. In each communication round of FL, the updated (locally or globally) ML model (or model differential when applicable) is transmitted over the noisy channel as described in Section III-B. Suppose that there are T total communication rounds and both the uplink and downlink total energy budget is $P = \sum_{t=1}^T P_t$, where P_t is the transmission power of the t -th round. We consider the following four schemes in the experiments.

- 1) **Noise free.** This is the ideal case where there is no noise in either uplink or downlink channels, i.e., the accurate model parameters are perfectly received at the server and clients. This represents the best-case performance.
- 2) **Equal power allocation.** In each communication round, the uplink and downlink average transmission power is the same, i.e., $P_t = P/T, \forall t = 1, \dots, T$. The received SNR of the model parameters is set as 10 dB in the experiments. This represents the current state of the art in [13].
- 3) **$\mathcal{O}(t^2)$ -increased power control policy.** Transmit power increases at the rate of $\mathcal{O}(t^2)$ with the communication rounds, i.e., the received SNR of the model parameters is increased and the effective

noise of the signal is decreased with the progress of FL. With the total budget P , it is straightforward to compute that $P_t = Pt^2/(T(T+1)(2T+1)), \forall t = 1, \dots, T$.

- 4) **$\mathcal{O}(t^2)$ -increased diversity combining policy.** The transmit power in both downlink and uplink remains the same. However, the final models at the server and clients of each communication round are obtained by multiple repeated transmissions and the subsequent combining. The number of the repeated transmissions increases at the rate of $\mathcal{O}(t^2)$. For simple discretization, we use 1, 4, 9, 16 and 25 orders of diversity combining in both uplink and downlink model transmissions for 1st to 9th, 10th to 45th, 46th to 125th, 125th to 270th, and 270th to 500th communication round, respectively, of a 500-round FEDAVG task. Note that the total transmit power budget in this scheme remains the same as the previous two methods.

We use the standard image classification and natural language processing FL tasks to evaluate the performances of these schemes. The following three standard datasets are used in the experiments, which are commonly accepted as the benchmark tasks to evaluate the performance of FL.

- 1) **MNIST.** The training sets contains 60000 examples. For the full clients participation case, the training sets are evenly distributed over $N = K = 10$ clients. For the partial clients participation case, the training sets are evenly partitioned over $N = 2000$ clients each containing 30 examples, and we set $K = 20$ per round (1% of total users). For the IID case, the data is shuffled and randomly assigned to each client, while for the non-IID case the data is sorted by labels and each client is then randomly assigned with 1 or 2 labels. The CNN model has two 5×5 convolution layers, a fully connected layer with 512 units and ReLU activation, and a final output layer with softmax. The first convolution layer has 32 channels while the second one has 64 channels, and both are followed by 2×2 max pooling. The following parameters are used for training: local batch size $BS = 5$, the number of local epochs $E = 1$, and learning rate $\eta = 0.065$.
- 2) **CIFAR-10.** We set $N = K = 10$ for the full clients participation case while $N = 100$ and $K = 10$ for the partial clients participation case. We train a CNN model with two 5×5 convolution layers (both with 64 channels), two fully connected layers (384 and 192 units respectively) with ReLU activation and a final output layer with softmax. The two convolution layers are both followed by 2×2 max pooling and a local response norm layer. The training parameters are: (a) IID: $BS = 50$, $E = 5$, learning rate initially sets to $\eta = 0.15$ and decays every 10 rounds with rate 0.99; (b) non-IID: $BS = 100$, $E = 1$, $\eta = 0.1$ and decay every round with rate 0.992.
- 3) **Shakespeare.** This dataset is built from *The Complete Works of William Shakespeare* and each speaking role is viewed as a client. Hence, the dataset is naturally unbalanced and non-IID since the number

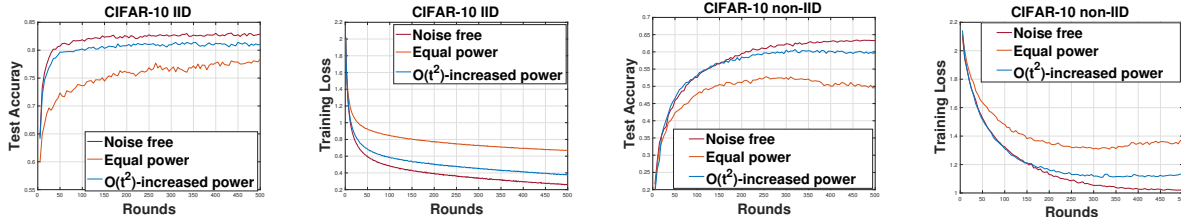


Fig. 2. Comparing the performance of transmit power control to the baselines with full clients participation, model transmission, and both IID (left two) and non-IID (right two) FL on the CIFAR-10 dataset.

of lines and speaking habits of each role vary significantly. There are totally 1129 roles in the dataset [44]. We randomly pick 300 of them and build a dataset with 794659 training examples and 198807 test examples. We also construct an IID dataset by shuffling the data and redistribute evenly to 300 roles and set $K = 10$. The ML task is the next-character prediction, and we use a classifier with an 8D embedding layer, two LSTM layers (each with 256 hidden units) and a softmax output layer with 86 nodes. The training parameters are: $BS = 20$, $E = 1$, learning rate initially sets to $\eta = 0.8$ and decays every 10 rounds with rate 0.99.

We compare the test accuracies and training losses as functions of the communication rounds for all the aforementioned configurations. All of the reported results are obtained by averaging over 5 independent runs. We also report the final test accuracy, which is averaged over the last 10 rounds, as the performance of the final global model.

B. Experiment Results for Transmit Power Control

We primarily evaluate the $\mathcal{O}(t^2)$ -increased transmit power control and compare with the noise free and equal power allocation baselines. The focus of the experiment is on partial clients participation under both MT and MDT, but we first report the results for full clients participation in CIFAR-10.

Full clients participation. We see from Fig. 2 that that under the same total power budget, the $\mathcal{O}(t^2)$ power control policy performs better than the equal power allocation scheme and is very close to the noise-free ideal case. Specifically, $\mathcal{O}(t^2)$ power control policy achieves 81.1% and 59.6% final test accuracy in IID and non-IID data partitions on CIFAR-10, which is 2.6% and 9.8% better than that of the equal power allocation scheme. Note that the training loss (test accuracy) of equal power allocation scheme increases (decreases) during the late rounds (350th to 500th) in the non-IID case, implying that a non-increasing SNR may occur deterioration in the convergence of FL for more difficult ML tasks. Similar results are also observed for MNIST and Shakespeare in the full clients participation case.

Partial clients participation. The performance comparisons of the the three schemes on MNIST, CIFAR-10 and Shakespeare datasets in both IID and non-IID configurations and MT are reported in

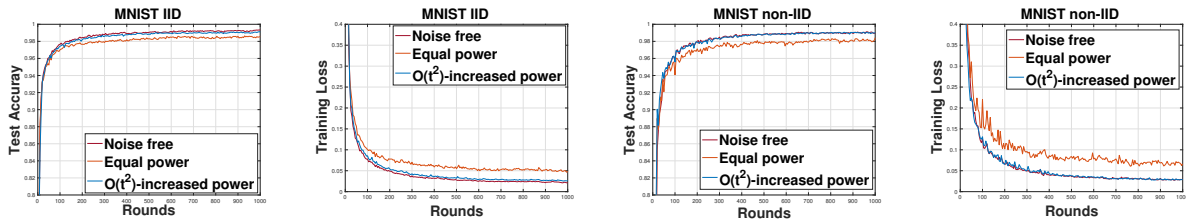


Fig. 3. Comparing the performance of transmit power control to the baselines with partial clients participation, model transmission, and both IID (left two) and non-IID (right two) FL on the MNIST dataset.

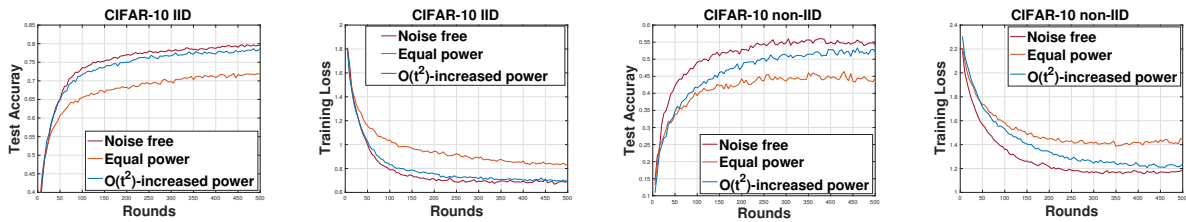


Fig. 4. Comparing the performance of transmit power control to the baselines with partial clients participation, model transmission, and both IID (left two) and non-IID (right two) FL on the CIFAR-10 dataset.

Figs. 3, 4, and 5, respectively. Their final model accuracies (after T rounds of FL are complete) are also summarized in Table I. First, we see from Fig. 3 that the proposed $\mathcal{O}(t^2)$ -increased power allocation scheme achieves higher test accuracy and lower train loss than the equal power allocation scheme under the same energy budget on MNIST. In particular, $\mathcal{O}(t^2)$ -increased power allocation scheme achieves 0.6% higher test accuracy than that of equal power allocation scheme in both IID and non-IID data partitions, respectively. It may seem that the gain is insignificant, but the reason is mostly due to that MNIST classification is a very simple task. In fact, the gain of power control is much more notable under the challenging CIFAR-10 and Shakespeare tasks as shown in Figs. 4 and Fig. 5, respectively. Compared with the equal power allocation scheme, which achieves 90.2% and 81.6% of the ideal (noise free) test accuracy in IID and non-IID data partitions under CIFAR-10 dataset respectively, the proposed $\mathcal{O}(t^2)$ -increased power allocation achieves 99.2% (IID) and 95.9% (non-IID) of the ideal (noise free) test accuracy respectively after $T = 500$ communication rounds. Similarly, under Shakespeare dataset, the

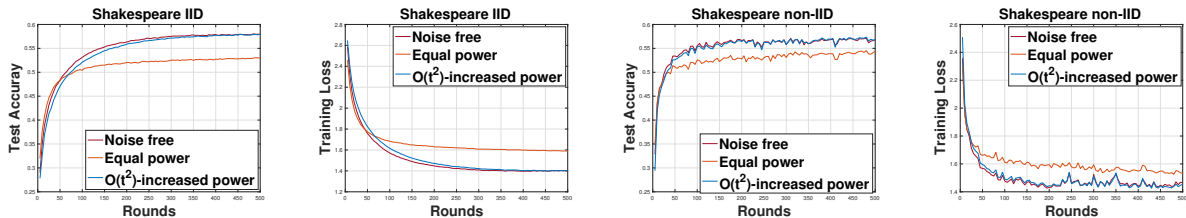


Fig. 5. Comparing the performance of transmit power control to the baselines with partial clients participation, model transmission, and both IID (left two) and non-IID (right two) FL on the Shakespeare dataset.

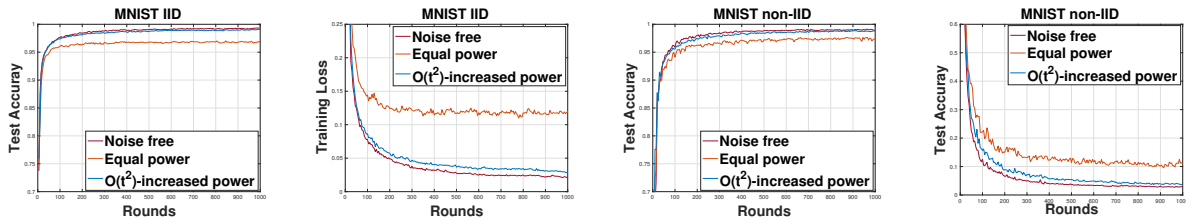


Fig. 6. Comparing the performance of transmit power control to the baselines with partial clients participation, model differential transmission, and both IID (left two) and non-IID (right two) FL on the MNIST dataset.

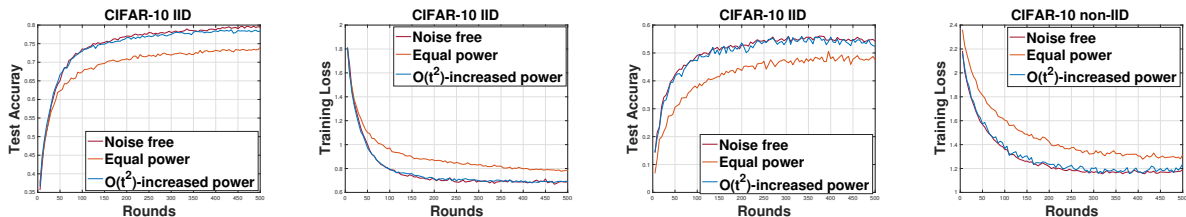


Fig. 7. Comparing the performance of transmit power control to the baselines with partial clients participation, model differential transmission, and both IID (left two) and non-IID (right two) FL on the CIFAR-10 dataset.

equal power allocation scheme achieves 91.5% (IID) and 95.8% (non-IID) of the ideal (noise free) test accuracy, while the proposed method improves 8.5% and 3.5%, respectively. Both tasks have significant accuracy improvement due to the $\mathcal{O}(t^2)$ power control.

MDT. We next present the experiment results of model differential transmission. Note that, by applying MDT, the uplink transmission power of the proposed scheme remains constant (recall that SNR is set as 10dB) while the downlink transmission power still increases at the rate of $\mathcal{O}(t^2)$. Figs. 6, 7 and 8 illustrate the test accuracies and training losses with MDT under MNIST, CIFAR-10 and Shakespeare datasets and the final model accuracies of the three schemes are summarized in Table II. We see that the proposed power control policy achieves 99.7% (99.7%), 99.2% (98.0%) and 100% (98.9%) of the ideal test accuracy in IID (non-IID) data setting under MNIST, CIFAR-10 and Shakespeare datasets, respectively, which significantly outperforms the baseline equal power allocation scheme.

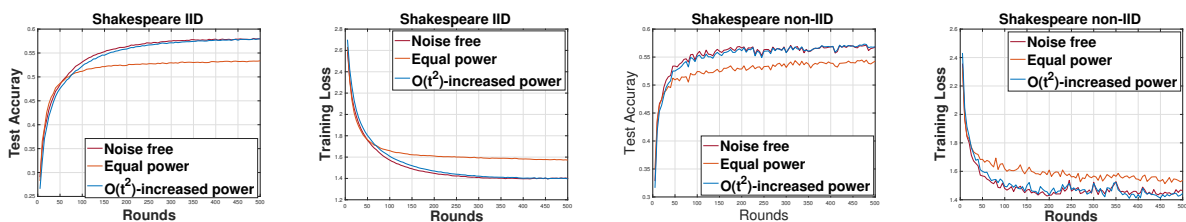


Fig. 8. Comparing the performance of transmit power control to the baselines with partial clients participation, model differential transmission, and both IID (left two) and non-IID (right two) FL on the Shakespeare dataset.

TABLE I
PERFORMANCE SUMMARY OF MODEL
TRANSMISSION (MT)

Dataset	Scheme	Accuracy		Percentage*	
		IID	non-IID	IID	non-IID
MNIST	Noise free	99.3%	100%	99.1%	100%
	Increased power	99.1%	99.8%	99.0%	99.9%
	Equal power	98.5%	99.2%	98.4%	99.3%
CIFAR-10	Noise free	79.5%	100%	54.3%	100%
	Increased power	78.9%	99.2%	52.1%	95.9%
	Equal power	71.7 %	90.2%	44.3%	81.6%
Shakespeare	Noise free	57.8%	100%	56.8%	100%
	Increased power	57.8%	100%	56.4%	99.3%
	Equal power	52.9 %	91.5%	54.4%	95.8%

TABLE II
PERFORMANCE SUMMARY OF MODEL
DIFFERENTIAL TRANSMISSION (MDT)

Dataset	Scheme	Accuracy		Percentage*	
		IID	non-IID	IID	non-IID
MNIST	Noise free	99.3%	100%	99.1%	100%
	Increased power	99.0%	99.7%	98.8%	99.7%
	Equal power	96.7%	97.4%	97.5%	98.4%
CIFAR-10	Noise free	79.5%	100%	54.3%	100%
	Increased power	78.9%	99.2%	53.2%	98.0%
	Equal power	73.9 %	93.0%	47.7%	87.8%
Shakespeare	Noise free	57.8%	100%	56.8%	100%
	Increased power	57.8%	100%	56.2%	98.9%
	Equal power	53.3 %	92.2%	54.3%	95.6%

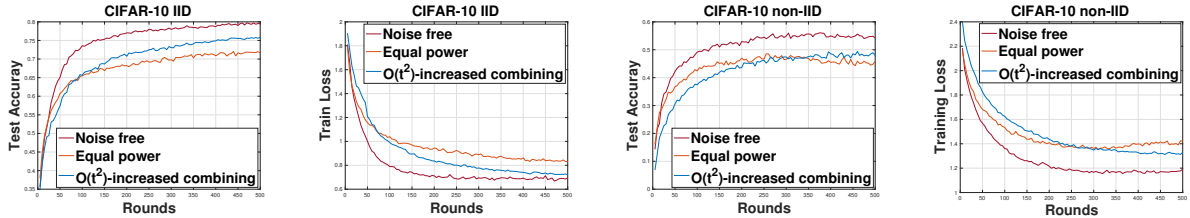


Fig. 9. Comparing the performance of diversity combining to the baselines with partial clients participation, model differential transmission, and both IID (left two) and non-IID (right two) FL on the CIFAR-10 dataset.

C. Experiment Results for Receiver Diversity Combining

We next evaluate the performance of diversity combining. Fig. 9 captures the test accuracies and training losses of diversity combining together with noise free and equal power allocation schemes. Although diversity combining is less flexible than the (continuous) transmit power control policy, we can see that it still outperforms the baseline method and approaches the noise-free ideal case. We notice that the training losses of diversity combining are larger than those of the equal power allocation scheme at the beginning stage of convergence, but as the diversity branches increase, the training losses eventually reduce and the model converges to a better global one. Particularly, diversity combining achieves 75.6% and 47.8% test accuracies for IID and non-IID data partitions, which is 3.9% and 3.4% better than the equal power allocation scheme.

VII. CONCLUSION

In this paper, we have investigated federated learning over noisy channels, where a FEDAVG pipeline with both uplink and downlink communication noises was studied. By theoretically analyzing the convergence of FL under noisy communications in both directions, we have proved that the same $\mathcal{O}(1/T)$ convergence rate of FEDAVG under perfect communications can be maintained if the uplink and downlink SNRs are controlled as $\mathcal{O}(t^2)$ over noisy channels for direct model transmission, and constant for model differential transmission. We have showcased two commonly used communication techniques – transmit

power control and diversity combining – to implement these theoretical results. Extensive experimental results have corroborated the theoretical analysis and demonstrated the performance superiority of the advanced transmit power control and diversity combining schemes over baseline methods under the same total energy budget.

APPENDIX A
PROOF OF THEOREM 1

A. Preliminaries

With a slight abuse of notation, we change the timeline to be with respect to the overall SGD iteration time steps instead of the communication rounds, i.e.,

$$t = \underbrace{1, \dots, E}_{\text{round 1}}, \underbrace{E+1, \dots, 2E}_{\text{round 2}}, \dots, \dots, \underbrace{(T-1)E+1, \dots, TE}_{\text{round } T}.$$

Note that the (noisy) global model \mathbf{w}_t is only accessible at the clients for specific $t \in \mathcal{I}_E$, where $\mathcal{I}_E = \{nE \mid n = 1, 2, \dots\}$, i.e., the time steps for communication. The notations for η_t , σ_t and ζ_t are similarly adjusted to this extended timeline, but their values remain the same inside the same round.

For client k , it trains the model with mini-batch SGD and we denote the one-step model update as:

$$\mathbf{v}_{t+1}^k = \mathbf{w}_t^k - \eta_t \nabla F_k(\mathbf{w}_t^k, \xi_t^k). \quad (29)$$

If $t+1 \notin \mathcal{I}_E$, the next-step result is $\mathbf{w}_{t+1}^k = \mathbf{v}_{t+1}^k$ since no global aggregation takes place. If $t+1 \in \mathcal{I}_E$, the server would receive the noisy weights $\tilde{\mathbf{w}}_{t+1}^k$ from all client $k \in [N]$. The global model is updated with $\mathbf{w}_{t+1} = \frac{1}{N} \sum_{k \in [N]} \tilde{\mathbf{w}}_{t+1}^k$ and then broadcast to all clients, who only receive the noisy global models $\hat{\mathbf{w}}_{t+1}^k = \mathbf{w}_{t+1} + \mathbf{e}_{t+1}^k$ due to the downlink communication errors. They then start the next local training period. We define the following variables that are used in the subsequent analysis:

$$\mathbf{u}_{t+1}^k \triangleq \begin{cases} \mathbf{v}_{t+1}^k & \text{if } t+1 \notin \mathcal{I}_E, \\ \frac{1}{N} \sum_{i \in [N]} \mathbf{v}_{t+1}^i & \text{if } t+1 \in \mathcal{I}_E; \end{cases}$$

$$\mathbf{p}_{t+1}^k \triangleq \begin{cases} \mathbf{v}_{t+1}^k & \text{if } t+1 \notin \mathcal{I}_E, \\ \mathbf{u}_{t+1}^k + \frac{1}{N} \sum_{i \in [N]} \mathbf{n}_{t+1}^i & \text{if } t+1 \in \mathcal{I}_E. \end{cases}$$

$$\mathbf{w}_{t+1}^k \triangleq \begin{cases} \mathbf{v}_{t+1}^k & \text{if } t+1 \notin \mathcal{I}_E, \\ \mathbf{p}_{t+1}^k + \mathbf{e}_{t+1}^k & \text{if } t+1 \in \mathcal{I}_E. \end{cases}$$

We define the following *virtual sequences*:

$$\bar{\mathbf{v}}_t = \frac{1}{N} \sum_{k=1}^N \mathbf{v}_t^k, \quad \bar{\mathbf{u}}_t = \frac{1}{N} \sum_{k=1}^N \mathbf{u}_t^k, \quad \bar{\mathbf{p}}_t = \frac{1}{N} \sum_{k=1}^N \mathbf{p}_t^k, \quad \text{and} \quad \bar{\mathbf{w}}_t = \frac{1}{N} \sum_{k=1}^N \mathbf{w}_t^k \quad (30)$$

to facilitate the analysis. We also define $\bar{\mathbf{g}}_t = \frac{1}{N} \sum_{k=1}^N \nabla F_k(\mathbf{w}_t^k)$ and $\mathbf{g}_t = \frac{1}{N} \sum_{k=1}^N \nabla F_k(\mathbf{w}_t^k, \zeta_t^k)$ for convenience. Therefore, $\bar{\mathbf{v}}_{t+1} = \bar{\mathbf{w}}_t - \eta_t \mathbf{g}_t$ and $\mathbb{E}[\mathbf{g}_t] = \bar{\mathbf{g}}_t$. We can also write the specific formulations of these virtual sequences when $t+1 \in \mathcal{I}_E$ as follows.

$$\bar{\mathbf{u}}_{t+1} = \frac{1}{N} \sum_{k=1}^N \mathbf{u}_{t+1}^k = \frac{1}{N} \sum_{i \in [N]} \mathbf{v}_{t+1}^i, \quad (31)$$

$$\bar{\mathbf{p}}_{t+1} = \frac{1}{N} \sum_{k=1}^N \mathbf{p}_{t+1}^k = \frac{1}{N} \sum_{k=1}^N \left[\mathbf{u}_{t+1}^k + \frac{1}{N} \sum_{i \in [N]} \mathbf{n}_{t+1}^i \right] = \bar{\mathbf{u}}_{t+1} + \frac{1}{N} \sum_{i \in [N]} \mathbf{n}_{t+1}^i, \quad (32)$$

$$\bar{\mathbf{w}}_{t+1} = \frac{1}{N} \sum_{k=1}^N \mathbf{w}_{t+1}^k = \frac{1}{N} \sum_{k=1}^N \left[\mathbf{p}_{t+1}^k + \mathbf{e}_{t+1}^k \right] = \bar{\mathbf{p}}_{t+1} + \frac{1}{N} \sum_{k=1}^N \mathbf{e}_{t+1}^k. \quad (33)$$

Note that for $t+1 \notin \mathcal{I}_E$, all these virtual sequences are the same. In addition, the global model (at the server) $\bar{\mathbf{p}}_{t+1}$ is meaningful only at $t+1 \in \mathcal{I}_E$. We emphasize that when $t+1 \in \mathcal{I}_E$, Eqns. (32) and (10) indicate that $\bar{\mathbf{p}}_{t+1} = \mathbf{w}_{t+1}$. Thus it is sufficient to analyze the convergence of $\|\bar{\mathbf{p}}_{t+1} - \mathbf{w}^*\|^2$ to prove Theorem 1.

B. Lemmas and proofs

Lemma 1. *Let Assumptions 1-1) to 4) hold, η_t is non-increasing, and $\eta_t \leq 2\eta_{t+E}$ for all $t \geq 0$. If $\eta_t \leq \frac{1}{4L}$, we have $\mathbb{E} \|\bar{\mathbf{v}}_{t+1} - \mathbf{w}^*\|^2 \leq (1 - \eta_t \mu) \mathbb{E} \|\bar{\mathbf{w}}_t - \mathbf{w}^*\|^2 + \eta_t^2 \left(\sum_{k=1}^N \frac{\delta_k^2}{N^2} + 6L\Gamma + 8(E-1)^2 H^2 \right)$.*

Lemma 1 establishes a bound for the one-step SGD. This result only concerns the local model update and is not impacted by the noisy communication. The proof can be constructed following the same steps as in [7], [23].

Lemma 2. *We have*

$$\mathbb{E} [\bar{\mathbf{p}}_{t+1}] = \bar{\mathbf{u}}_{t+1}, \quad \mathbb{E} \|\bar{\mathbf{u}}_{t+1} - \bar{\mathbf{p}}_{t+1}\|^2 = \frac{d\sigma_{t+1}^2}{N^2}, \quad (34)$$

and

$$\mathbb{E} [\bar{\mathbf{w}}_{t+1}] = \bar{\mathbf{p}}_{t+1}, \quad \mathbb{E} \|\bar{\mathbf{w}}_{t+1} - \bar{\mathbf{p}}_{t+1}\|^2 = \frac{d\zeta_{t+1}^2}{N^2}, \quad (35)$$

for $t+1 \in \mathcal{I}_E$, where $\sigma_{t+1}^2 \triangleq \sum_{k \in [N]} \sigma_{t+1,k}^2$ and $\zeta_{t+1}^2 \triangleq \sum_{k \in [N]} \zeta_{t+1,k}^2$.

Proof. For $t + 1 \in \mathcal{I}_E$, according to (32), we have $\mathbb{E} [\bar{\mathbf{p}}_{t+1} - \bar{\mathbf{u}}_{t+1}] = \frac{1}{K} \sum_{k \in [N]} \mathbb{E} [\mathbf{n}_{t+1}^k] = \mathbf{0}$. and

$$\mathbb{E} \|\bar{\mathbf{p}}_{t+1} - \bar{\mathbf{u}}_{t+1}\|^2 = \frac{1}{N^2} \mathbb{E} \left\| \sum_{k \in [N]} \mathbf{n}_{t+1}^k \right\|^2 = \frac{1}{N^2} \sum_{k \in [N]} \mathbb{E} \|\mathbf{n}_{t+1}^k\|^2 = \frac{\sum_{k \in [N]} d\sigma_{t+1,k}^2}{N^2} = \frac{d\sigma_{t+1}^2}{N^2}$$

because $\{\mathbf{n}_{t+1}^k, \forall k\}$ are independent variables. Similarly, according to (33), we have $\mathbb{E} [\bar{\mathbf{w}}_{t+1} - \bar{\mathbf{p}}_{t+1}] = \frac{1}{N} \sum_{k \in [N]} \mathbb{E} [\mathbf{e}_{t+1}^k] = \mathbf{0}$ and

$$\mathbb{E} \|\bar{\mathbf{w}}_{t+1} - \bar{\mathbf{p}}_{t+1}\|^2 = \frac{1}{N^2} \mathbb{E} \left\| \sum_{k \in [N]} \mathbf{e}_{t+1}^k \right\|^2 = \frac{1}{N^2} \sum_{k \in [N]} \mathbb{E} \|\mathbf{e}_{t+1}^k\|^2 = \frac{\sum_{k \in [N]} d\zeta_{t+1,k}^2}{N^2} = \frac{d\zeta_{t+1}^2}{N^2}.$$

□

C. Proof of Theorem

We need to consider four cases for the analysis of the convergence of $\mathbb{E} \|\bar{\mathbf{p}}_{t+1} - \mathbf{w}^*\|^2$.

1) If $t \notin \mathcal{I}_E$ and $t + 1 \notin \mathcal{I}_E$, $\bar{\mathbf{w}}_t = \bar{\mathbf{p}}_t$ and $\bar{\mathbf{v}}_{t+1} = \bar{\mathbf{p}}_{t+1}$. Using Lemma 1, we have:

$$\begin{aligned} \mathbb{E} \|\bar{\mathbf{p}}_{t+1} - \mathbf{w}^*\|^2 &= \mathbb{E} \|\bar{\mathbf{v}}_{t+1} - \mathbf{w}^*\|^2 \\ &\leq (1 - \eta_t \mu) \mathbb{E} \|\bar{\mathbf{p}}_t - \mathbf{w}^*\|^2 + \eta_t^2 \left[\sum_{k=1}^N \frac{\delta_k^2}{N^2} + 6L\Gamma + 8(E-1)^2 H^2 \right]. \end{aligned} \quad (36)$$

2) If $t \in \mathcal{I}_E$ and $t + 1 \notin \mathcal{I}_E$, we still have $\bar{\mathbf{v}}_{t+1} = \bar{\mathbf{p}}_{t+1}$. Note that we have $\bar{\mathbf{w}}_t = \bar{\mathbf{p}}_t + \frac{1}{N} \sum_{k=1}^N \mathbf{e}_t^k$. Then:

$$\|\bar{\mathbf{w}}_t - \mathbf{w}^*\|^2 = \|\bar{\mathbf{w}}_t - \bar{\mathbf{p}}_t + \bar{\mathbf{p}}_t - \mathbf{w}^*\|^2 = \|\bar{\mathbf{p}}_t - \mathbf{w}^*\|^2 + \underbrace{\|\bar{\mathbf{w}}_t - \bar{\mathbf{p}}_t\|^2}_{A_1} + \underbrace{2\langle \bar{\mathbf{w}}_t - \bar{\mathbf{p}}_t, \bar{\mathbf{p}}_t - \mathbf{w}^* \rangle}_{A_2}.$$

We first note that the expectation of A_2 over the noise randomness is zero since we have $\mathbb{E} [\bar{\mathbf{w}}_t - \bar{\mathbf{p}}_t] = \mathbf{0}$ (from Eqn. (35)). Second, the expectation of A_1 can be bounded using Lemma 2. We then have

$$\begin{aligned} \mathbb{E} \|\bar{\mathbf{p}}_{t+1} - \mathbf{w}^*\|^2 &= \mathbb{E} \|\bar{\mathbf{v}}_{t+1} - \mathbf{w}^*\|^2 \\ &\leq (1 - \eta_t \mu) \mathbb{E} \|\bar{\mathbf{p}}_t - \mathbf{w}^*\|^2 + (1 - \eta_t \mu) \mathbb{E} \|\bar{\mathbf{w}}_t - \bar{\mathbf{p}}_t\|^2 + \eta_t^2 \left[\frac{\delta_k^2}{N^2} + 6L\Gamma + 8(E-1)^2 H^2 \right] \\ &\leq (1 - \eta_t \mu) \mathbb{E} \|\bar{\mathbf{p}}_t - \mathbf{w}^*\|^2 + (1 - \eta_t \mu) \frac{d\zeta_t^2}{N^2} + \eta_t^2 \left[\sum_{k=1}^N \frac{\delta_k^2}{N^2} + 6L\Gamma + 8(E-1)^2 H^2 \right]. \end{aligned} \quad (37)$$

3) If $t \notin \mathcal{I}_E$ and $t + 1 \in \mathcal{I}_E$, then we still have $\bar{\mathbf{w}}_t = \bar{\mathbf{p}}_t$. For $t + 1$, we need to evaluate the convergence

of $\mathbb{E} \|\bar{\mathbf{p}}_{t+1} - \mathbf{w}^*\|^2$. We have

$$\begin{aligned} \|\bar{\mathbf{p}}_{t+1} - \mathbf{w}^*\|^2 &= \|\bar{\mathbf{p}}_{t+1} - \bar{\mathbf{u}}_{t+1} + \bar{\mathbf{u}}_{t+1} - \mathbf{w}^*\|^2 \\ &= \underbrace{\|\bar{\mathbf{p}}_{t+1} - \bar{\mathbf{u}}_{t+1}\|^2}_{B_1} + \underbrace{\|\bar{\mathbf{u}}_{t+1} - \mathbf{w}^*\|^2}_{B_2} + 2 \underbrace{\langle \bar{\mathbf{p}}_{t+1} - \bar{\mathbf{u}}_{t+1}, \bar{\mathbf{u}}_{t+1} - \mathbf{w}^* \rangle}_{B_3}. \end{aligned} \quad (38)$$

We first note that the expectation of B_3 over the noise is zero since we have $\mathbb{E} [\bar{\mathbf{u}}_{t+1} - \bar{\mathbf{p}}_{t+1}] = \mathbf{0}$ (from Eqn. (34)). Second, the expectation of B_1 can be bounded using Lemma 2. Noticing that $\bar{\mathbf{u}}_{t+1} = \bar{\mathbf{v}}_{t+1}$ for B_2 and applying Lemma 1, we have:

$$\begin{aligned} \mathbb{E} \|\bar{\mathbf{p}}_{t+1} - \mathbf{w}^*\|^2 &\leq \mathbb{E} \|\bar{\mathbf{v}}_{t+1} - \mathbf{w}^*\|^2 + \frac{d\sigma_{t+1}^2}{K^2} \\ &\leq (1 - \eta_t \mu) \mathbb{E} \|\bar{\mathbf{p}}_t - \mathbf{w}^*\|^2 + \frac{d\sigma_{t+1}^2}{N^2} + \eta_t^2 \left[\sum_{k=1}^N \frac{\delta_k^2}{N^2} + 6L\Gamma + 8(E-1)^2 H^2 \right]. \end{aligned} \quad (39)$$

4) If $t \in \mathcal{I}_E$ and $t+1 \in \mathcal{I}_E$, $\bar{\mathbf{v}}_{t+1} \neq \bar{\mathbf{p}}_{t+1}$ and $\bar{\mathbf{w}}_t \neq \bar{\mathbf{p}}_t$. (Note that this is possible only for $E = 1$.)

Combining the results from the previous two cases, we have

$$\mathbb{E} \|\bar{\mathbf{p}}_{t+1} - \mathbf{w}^*\|^2 \leq (1 - \eta_t \mu) \mathbb{E} \|\bar{\mathbf{p}}_t - \mathbf{w}^*\|^2 + (1 - \eta_t \mu) \frac{d\zeta_t^2}{N^2} + \frac{d\sigma_{t+1}^2}{N^2} + \eta_t^2 \left[\sum_{k=1}^N \frac{\delta_k^2}{N^2} + 6L\Gamma + 8(E-1)^2 H^2 \right]. \quad (40)$$

Finally, we have that inequality (40) holds for all four cases. Denote $\Delta_t = \mathbb{E} \|\bar{\mathbf{p}}_t - \mathbf{w}^*\|^2$. If we set the effective noise power σ_{t+1}^2 and ζ_t^2 such that $\sigma_{t+1}^2 \leq N^2 \eta_t^2$ and $\zeta_t^2 \leq N^2 \frac{\eta_t^2}{1 - \eta_t \mu}$, we always have

$$\Delta_{t+1} \leq (1 - \eta_t \mu) \Delta_t + \eta_t^2 D,$$

where $D = \sum_{k=1}^N \frac{\delta_k^2}{N^2} + 6L\Gamma + 8(E-1)^2 H^2 + 2d$. We decay the learning rate as $\eta_t = \frac{\beta}{t+\gamma}$ for some $\beta \geq \frac{1}{\mu}$ and $\gamma \geq 0$ such that $\eta_1 \leq \min\{\frac{1}{\mu}, \frac{1}{4L}\} = \frac{1}{4L}$ and $\eta_t \leq 2\eta_{t+E}$. Now we prove that $\Delta_t \leq \frac{v}{\gamma+t}$ where $v = \max\{\frac{\beta^2 D}{\beta\mu-1}, (\gamma+1)\Delta_0\}$ by induction. First, the definition of v ensures that it holds for $t = 0$.

Assume the conclusion holds for some $t > 0$. It then follows that

$$\begin{aligned} \Delta_{t+1} &\leq (1 - \eta_t \mu) \Delta_t + \eta_t^2 D = \left(1 - \frac{\beta\mu}{t+\gamma}\right) \frac{v}{t+\gamma} + \frac{\beta^2 D}{(t+\gamma)^2} \\ &= \frac{t+\gamma-1}{(t+\gamma)^2} v + \left[\frac{\beta^2 D}{(t+\gamma)^2} - \frac{\mu\beta-1}{(t+\gamma)^2} v \right] \leq \frac{v}{t+\gamma+1}. \end{aligned}$$

Specially, if we choose $\beta = \frac{2}{\mu}$, $\gamma = \max\{8\frac{L}{\mu} - 1, E\}$ and denote $\kappa = \frac{L}{\mu}$, then $\eta_t = \frac{2}{\mu} \frac{1}{\gamma+t}$. Using $\max\{a, b\} \leq a + b$, we have $v \leq \frac{4D}{\mu^2} + (\gamma+1)\Delta_0 \leq \frac{4D}{\mu^2} + (8\kappa + E) \|\mathbf{w}_0 - \mathbf{w}^*\|^2$. Therefore, $\Delta_t \leq \frac{v}{\gamma+t} = \frac{1}{\gamma+t} \left[\frac{4D}{\mu^2} + (8\kappa + E) \|\mathbf{w}_0 - \mathbf{w}^*\|^2 \right]$. Setting $t = T$ concludes the proof.

APPENDIX B
PROOF OF THEOREM 2

The additional difficulty in proving Theorem 2 comes from partial clients participation. The approach we take is to study a “virtual” FL process where *all clients* receive the noisy downlink broadcast of the latest global model, and they all participate in the subsequent local model update phase. However, only the selected clients in \mathcal{S}_{t+1} upload their updated local model to the server via the noisy uplink channel. It is clear that this “virtual” FL is equivalent to the original process in terms of the convergence – clients that are not selected do not contribute to the global model aggregation. This seemingly redundant process, however, circumvents the difficulty due to partial clients participation as can be seen in the analysis.

Before presenting the proof, we first elaborate on some necessary changes of notation. The notation defined in Section A-A can be largely reused, with the notable distinction that now we have to separate the cases for K and for N . The variables of \mathbf{u}_{t+1}^k and \mathbf{p}_{t+1}^k are now defined as:

$$\mathbf{u}_{t+1}^k \triangleq \begin{cases} \mathbf{v}_{t+1}^k & \text{if } t+1 \notin \mathcal{I}_E, \\ \frac{1}{K} \sum_{i \in \mathcal{S}_t} \mathbf{v}_{t+1}^i & \text{if } t+1 \in \mathcal{I}_E; \end{cases}$$

$$\mathbf{p}_{t+1}^k \triangleq \begin{cases} \mathbf{v}_{t+1}^k & \text{if } t+1 \notin \mathcal{I}_E, \\ \mathbf{u}_{t+1}^k + \frac{1}{K} \sum_{i \in \mathcal{S}_t} \mathbf{n}_{t+1}^i & \text{if } t+1 \in \mathcal{I}_E. \end{cases}$$

Note that Lemma 2 still holds with the following update: $\mathbb{E} \|\bar{\mathbf{u}}_{t+1} - \bar{\mathbf{p}}_{t+1}\|^2 = \frac{d\bar{\sigma}_{t+1}^2}{K}$, $\mathbb{E} \|\bar{\mathbf{w}}_{t+1} - \bar{\mathbf{p}}_{t+1}\|^2 = \frac{d\bar{\zeta}_{t+1}^2}{N}$. In addition, we need the following lemma, whose proof is omitted due to space limitation.

Lemma 3. *Let Assumption 1-4) hold. Also assume that $\eta_t \leq 2\eta_{t+E}$ for all $t \geq 0$. Then for $t+1 \in \mathcal{I}_E$, we have*

$$\mathbb{E} [\bar{\mathbf{u}}_{t+1}] = \bar{\mathbf{v}}_{t+1}, \quad \text{and} \quad \mathbb{E} \|\bar{\mathbf{v}}_{t+1} - \bar{\mathbf{u}}_{t+1}\|^2 \leq \frac{N-K}{N-1} \frac{4}{K} \eta_t^2 E^2 H^2. \quad (41)$$

We can now similarly analyze the four cases as in Section A-C. Cases 1) and 2) remain the same as before. For Case 3) we need to consider $t \notin \mathcal{I}_E$ and $t+1 \in \mathcal{I}_E$. Note that Eqn. (38) still holds, but we need to re-evaluate the expectation of B_2 because of partial clients participation. We have:

$$\begin{aligned} \|\bar{\mathbf{u}}_{t+1} - \mathbf{w}^*\|^2 &= \|\bar{\mathbf{u}}_{t+1} - \bar{\mathbf{v}}_{t+1} + \bar{\mathbf{v}}_{t+1} - \mathbf{w}^*\|^2 \\ &= \underbrace{\|\bar{\mathbf{u}}_{t+1} - \bar{\mathbf{v}}_{t+1}\|^2}_{C_1} + \underbrace{\|\bar{\mathbf{v}}_{t+1} - \mathbf{w}^*\|^2}_{C_2} + 2 \underbrace{\langle \bar{\mathbf{u}}_{t+1} - \bar{\mathbf{v}}_{t+1}, \bar{\mathbf{v}}_{t+1} - \mathbf{w}^* \rangle}_{C_3}. \end{aligned} \quad (42)$$

When the expectation is taken over the random clients sampling, the expectation of C_3 is zero since we have $\mathbb{E} [\bar{\mathbf{u}}_{t+1} - \bar{\mathbf{v}}_{t+1}] = \mathbf{0}$ (from Eqn. (41)). The expectation of C_1 can be bounded using Lemma 3.

Therefore we have $\mathbb{E} \|\bar{\mathbf{p}}_{t+1} - \mathbf{w}^*\|^2 \leq \mathbb{E} \|\bar{\mathbf{v}}_{t+1} - \mathbf{w}^*\|^2 + \frac{d\bar{\sigma}_{t+1}^2}{K} + \frac{N-K}{N-1} \frac{4}{K} \eta_t^2 E^2 H^2$. Using Lemma 1, we have

$$\begin{aligned} \mathbb{E} \|\bar{\mathbf{p}}_{t+1} - \mathbf{w}^*\|^2 &\leq \mathbb{E} \|\bar{\mathbf{v}}_{t+1} - \mathbf{w}^*\|^2 + \frac{d\bar{\sigma}_{t+1}^2}{K} + \frac{N-K}{N-1} \frac{4}{K} \eta_t^2 E^2 H^2 \\ &\leq (1 - \eta_t \mu) \mathbb{E} \|\bar{\mathbf{p}}_t - \mathbf{w}^*\|^2 + \frac{d\bar{\sigma}_{t+1}^2}{K} + \eta_t^2 \left[\sum_{k=1}^N \frac{\delta_k^2}{N^2} + 6L\Gamma + 8(E-1)^2 H^2 + \frac{N-K}{N-1} \frac{4}{K} E^2 H^2 \right]. \end{aligned}$$

Case 4) should be similarly updated based on the new result in Case 3). Finally, we have that

$$\begin{aligned} \mathbb{E} \|\bar{\mathbf{p}}_{t+1} - \mathbf{w}^*\|^2 &\leq (1 - \eta_t \mu) \mathbb{E} \|\bar{\mathbf{p}}_t - \mathbf{w}^*\|^2 + (1 - \eta_t \mu) \frac{d\bar{\zeta}_t^2}{N} + \frac{d\bar{\sigma}_{t+1}^2}{K} \\ &\quad + \eta_t^2 \left[\sum_{k=1}^N \frac{\delta_k^2}{N^2} + 6L\Gamma + 8(E-1)^2 H^2 + \frac{N-K}{N-1} \frac{4}{K} E^2 H^2 \right] \end{aligned} \quad (43)$$

holds for all cases. If we set $\bar{\sigma}_{t+1}^2$ and $\bar{\zeta}_t^2$ such that $\bar{\sigma}_{t+1}^2 \leq K\eta_t^2$ and $\bar{\zeta}_t^2 \leq N \frac{\eta_t^2}{1-\eta_t\mu}$, the remaining proof follows the same way as in Section A-C.

APPENDIX C

PROOF OF THEOREM 3

For model differential transmission (MDT), if $t+1 \in \mathcal{I}_E$, the global aggregation is given in Eqn. (11). Similar to Appendix A and B, we expand the timeline to be with respect to the overall SGD iteration time steps, and define the following variables to facilitate the proof. $\mathbf{v}_{t+1}^k \triangleq \mathbf{w}_t^k - \eta_t \nabla F_k(\mathbf{w}_t^k, \xi_t^k)$, $\mathbf{d}_{t+1}^k \triangleq \mathbf{v}_{t+1}^k - \mathbf{w}_{t+1-E}^k$. Furthermore, when $t+1 \notin \mathcal{I}_E$ we define $\mathbf{u}_{t+1}^k = \mathbf{p}_{t+1}^k = \mathbf{w}_{t+1}^k \triangleq \mathbf{v}_{t+1}^k$, and when $t+1 \in \mathcal{I}_E$ we define $\mathbf{u}_{t+1}^k \triangleq \frac{1}{K} \sum_{i \in \mathcal{S}_t} \mathbf{v}_{t+1}^i$, $\mathbf{p}_{t+1}^k \triangleq \mathbf{w}_{t+1-E}^k + \frac{1}{K} \sum_{i \in \mathcal{S}_t} [\mathbf{d}_{t+1}^i + \mathbf{n}_{t+1}^i]$, and $\mathbf{w}_{t+1}^k \triangleq \mathbf{p}_{t+1}^k + \mathbf{e}_{t+1}^k$. The virtual sequences $\bar{\mathbf{v}}_t$, $\bar{\mathbf{u}}_t$, $\bar{\mathbf{p}}_t$ and $\bar{\mathbf{w}}_t$ remain the same as Eqn. (30). $\bar{\mathbf{g}}_t$ and $\bar{\mathbf{g}}_t$ are also similarly defined. Note that the global model at the server is the same as $\bar{\mathbf{p}}_t$, i.e., $\mathbf{w}_{t+1} = \bar{\mathbf{p}}_{t+1}$.

We first establish the follow in lemma, which is instrumental in the proof of Theorem 3.

Lemma 4. *Let Assumption 1-4) hold. Assume that $\eta_t \leq 2\eta_{t+E}$ for all $t \geq 0$, and further assume that the uplink communication adopts a constant SNR control policy: $\text{SNR}_{t,k}^{S,MDT} = \nu$. Then, for $t+1 \in \mathcal{I}_E$, we have: $\mathbb{E} [\bar{\mathbf{p}}_{t+1}] = \bar{\mathbf{u}}_{t+1}$, $\mathbb{E} \|\bar{\mathbf{u}}_{t+1} - \bar{\mathbf{p}}_{t+1}\|^2 \leq (1 + \frac{1}{\nu}) \frac{d}{K} \bar{\zeta}_{t+1-E}^2 + \frac{4E^2}{K\nu} \eta_t^2 H^2$.*

Proof. Note that if $t+1 \in \mathcal{I}_E$, so does $t+1-E$. Insert $\mathbf{d}_{t+1}^k = \mathbf{v}_{t+1}^k - \mathbf{w}_{t+1-E}^k$ into \mathbf{p}_{t+1}^k , we have $\mathbb{E} [\bar{\mathbf{p}}_{t+1}] = \bar{\mathbf{u}}_{t+1} + \frac{1}{K} \mathbb{E} [\sum_{k \in \mathcal{S}_t} \mathbf{n}_{t+1}^k] - \frac{1}{K} \mathbb{E} [\sum_{k \in \mathcal{S}_t} \mathbf{e}_{t+1-E}^k] = \mathbb{E} [\bar{\mathbf{u}}_{t+1}]$. As for the variance, we have

$$\mathbb{E} \|\bar{\mathbf{u}}_{t+1} - \bar{\mathbf{p}}_{t+1}\|^2 = \frac{1}{K^2} \mathbb{E} \left\| \sum_{k \in \mathcal{S}_t} \mathbf{n}_{t+1}^k \right\|^2 + \frac{1}{K^2} \mathbb{E} \left\| \sum_{k \in \mathcal{S}_t} \mathbf{e}_{t+1-E}^k \right\|^2 = \frac{1}{K^2 \nu} \mathbb{E} \left\| \sum_{k \in \mathcal{S}_t} \mathbf{d}_{t+1}^k \right\|^2 + \frac{d\bar{\zeta}_{t+1-E}^2}{K} \quad (44)$$

where the last equality comes from the constant uplink SNR control, Eqn. (9), and the assumption that each client has the same downlink noise power $\bar{\zeta}_t^2$, $\forall k \in [N]$. We further have

$$\begin{aligned} \mathbb{E} \left\| \sum_{k \in \mathcal{S}_t} \mathbf{d}_{t+1}^k \right\|^2 &= \mathbb{E} \left\| \sum_{k \in \mathcal{S}_t} (\mathbf{v}_{t+1}^k - \mathbf{w}_{t+1-E}) \right\|^2 + dK\bar{\zeta}_{t+1-E}^2 \\ &\leq \mathbb{E}_{\mathcal{S}_t} \left[\sum_{k \in \mathcal{S}_t} \mathbb{E}_{\text{SG}} \left\| \sum_{\tau=t+1-E}^t \eta_\tau \nabla F_k(\mathbf{w}_\tau^k, \xi_\tau^k) \right\|^2 \right] + dK\bar{\zeta}_{t+1-E}^2 \leq 4E^2 K \eta_t^2 H^2 + dK\bar{\zeta}_{t+1-E}^2 \end{aligned} \quad (45)$$

using the Cauchy-Schwarz inequality, Assumption 1-4), and $\eta_{t+1-E} < \eta_{t-E} \leq 2\eta_t$. Plugging Eqn. (45) back to Eqn. (44) gives

$$\mathbb{E} \|\bar{\mathbf{u}}_{t+1} - \bar{\mathbf{p}}_{t+1}\|^2 = \frac{1}{K^2\nu} \mathbb{E} \left\| \sum_{k \in \mathcal{S}_{t+1}} \mathbf{d}_{t+1}^k \right\|^2 + \frac{d\bar{\zeta}_{t+1-E}^2}{K} \leq \left(1 + \frac{1}{\nu}\right) \frac{d}{K} \bar{\zeta}_{t+1-E}^2 + \frac{4E^2}{K\nu} \eta_t^2 H^2,$$

which completes the proof. \square

We are now ready to present the proof of Theorem 3, which is similar to that of Theorem 2. In particular, the analysis of four cases in Section B still hold, with the only change that Eqn. (43) is updated to Eqn. (46) below using Lemma 4.

$$\begin{aligned} \mathbb{E} \|\bar{\mathbf{p}}_{t+1} - \mathbf{w}^*\|^2 &\leq (1 - \eta_t \mu) \mathbb{E} \|\bar{\mathbf{p}}_t - \mathbf{w}^*\|^2 + (1 - \eta_t \mu) \frac{d}{N} \bar{\zeta}_t^2 + \left(1 + \frac{1}{\nu}\right) \frac{d}{K} \bar{\zeta}_t^2 \\ &\quad + \eta_t^2 \left[\sum_{k=1}^N \frac{\delta_k^2}{N^2} + 6L\Gamma + 8(E-1)^2 H^2 + \frac{N-K}{N-1} \frac{4}{K} E^2 H^2 + \frac{4E^2}{K\nu} H^2 \right]. \end{aligned} \quad (46)$$

We note that the constant uplink SNR control is already used in Lemma 4 and Eqn. (46). Then, by the definition of $\Delta_t = \mathbb{E} \|\bar{\mathbf{p}}_t - \mathbf{w}^*\|^2$ and controlling the downlink SNR such that $\bar{\zeta}_t^2 \leq \frac{NK\eta_t^2}{(1-\eta_t\mu)K + (1+\frac{1}{\nu})N}$, we have

$$\Delta_{t+1} \leq (1 - \eta_t \mu) \Delta_t + \eta_t^2 D$$

where

$$D \triangleq \sum_{k=1}^N \frac{\delta_k^2}{N^2} + 6L\Gamma + 8(E-1)^2 H^2 + \frac{N-K}{N-1} \frac{4}{K} E^2 H^2 + \frac{4E^2}{K\nu} H^2 + d.$$

The remaining proof follows the same induction steps as in Appendix A and B.

REFERENCES

- [1] B. McMahan, E. Moore, D. Ramage, S. Hampson, and B. A. y Arcas, "Communication-efficient learning of deep networks from decentralized data," in *Proc. AISTATS*, Apr. 2017, pp. 1273–1282.
- [2] J. Konecny, H. B. McMahan, F. X. Yu, P. Richtarik, A. T. Suresh, and D. Bacon, "Federated learning: Strategies for improving communication efficiency," in *NIPS Workshop on Private Multi-Party Machine Learning*, 2016.

- [3] K. Bonawitz *et al.*, “Towards federated learning at scale: System design,” in *Proc. SysML Conference*, 2019, pp. 1–15.
- [4] P. Kairouz *et al.*, “Advances and open problems in federated learning,” *arXiv preprint arXiv:1912.04977*, 2019.
- [5] T. Li, A. K. Sahu, A. Talwalkar, and V. Smith, “Federated learning: Challenges, methods, and future directions,” *IEEE Signal Process. Mag.*, vol. 37, no. 3, pp. 50–60, 2020.
- [6] T. Li, A. K. Sahu, M. Zaheer, M. Sanjabi, A. Talwalkar, and V. Smith, “Federated optimization in heterogeneous networks,” in *Proceedings of the 3rd MLSys Conference*, 2020.
- [7] S. Zheng, C. Shen, and X. Chen, “Design and analysis of uplink and downlink communications for federated learning,” *IEEE J. Select. Areas Commun.*, 2020, to appear.
- [8] A. Reiszadeh, A. Mokhtari, H. Hassani, A. Jadbabaie, and R. Pedarsani, “FedPAQ: A communication-efficient federated learning method with periodic averaging and quantization,” in *Proc. AISTATS*, 2020.
- [9] Y. Du, S. Yang, and K. Huang, “High-dimensional stochastic gradient quantization for communication-efficient edge learning,” *IEEE Trans. Signal Processing*, vol. 68, pp. 2128–2142, 2020.
- [10] W. Y. B. Lim, N. C. Luong, D. T. Hoang, Y. Jiao, Y.-C. Liang, Q. Yang, D. Niyato, and C. Miao, “Federated learning in mobile edge networks: A comprehensive survey,” *IEEE Commun. Surveys Tuts.*, 2020.
- [11] G. Zhu, D. Liu, Y. Du, C. You, J. Zhang, and K. Huang, “Toward an intelligent edge: Wireless communication meets machine learning,” *IEEE Commun. Mag.*, vol. 58, no. 1, pp. 19–25, 2020.
- [12] Q. Zeng, Y. Du, K. K. Leung, and K. Huang, “Energy-efficient radio resource allocation for federated edge learning,” *arXiv preprint arXiv:1907.06040*, 2019.
- [13] G. Zhu, Y. Wang, and K. Huang, “Broadband analog aggregation for low-latency federated edge learning,” *IEEE Trans. Wireless Commun.*, vol. 19, no. 1, pp. 491–506, 2019.
- [14] X. Cao, G. Zhu, J. Xu, and S. Cui, “Optimized power control for over-the-air federated edge learning,” *arXiv preprint arXiv:2011.05587*, 2020.
- [15] M. Chen, Z. Yang, W. Saad, C. Yin, H. V. Poor, and S. Cui, “A joint learning and communications framework for federated learning over wireless networks,” *arXiv preprint arXiv:1909.07972*, 2019.
- [16] T. Nishio and R. Yonetani, “Client selection for federated learning with heterogeneous resources in mobile edge,” in *IEEE International Conference on Communications (ICC)*. IEEE, 2019, pp. 1–7.
- [17] W. Shi, S. Zhou, and Z. Niu, “Device scheduling with fast convergence for wireless federated learning,” *arXiv preprint arXiv:1911.00856*, 2019.
- [18] J. Xu and H. Wang, “Client selection and bandwidth allocation in wireless federated learning networks: A long-term perspective,” *IEEE Trans. Wireless Commun.*, pp. 1–1, 2020.
- [19] M. M. Amiri, D. Gunduz, S. R. Kulkarni, and H. V. Poor, “Federated learning with quantized global model updates,” *arXiv preprint arXiv:2006.10672*, 2020.
- [20] S. U. Stich, “Local SGD converges fast and communicates little,” in *Proc. ICLR*, 2018.
- [21] J. Wang and G. Joshi, “Cooperative SGD: A unified framework for the design and analysis of communication-efficient SGD algorithms,” in *ICML Workshop on Coding Theory for Machine Learning*, 2019.
- [22] F. Haddadpour, M. M. Kamani, M. Mahdavi, and V. Cadambe, “Local SGD with periodic averaging: Tighter analysis and adaptive synchronization,” in *Advances in Neural Information Processing Systems*, 2019, pp. 11 080–11 092.
- [23] X. Li, K. Huang, W. Yang, S. Wang, and Z. Zhang, “On the convergence of FedAvg on non-IID data,” in *International Conference on Learning Representations*, 2020.
- [24] A. Bhowmick, J. Duchi, J. Freudiger, G. Kapoor, and R. Rogers, “Protection against reconstruction and its applications in private federated learning,” *arXiv preprint arXiv:1812.00984*, 2018.

- [25] C. Niu, F. Wu, S. Tang, L. Hua, R. Jia, C. Lv, Z. Wu, and G. Chen, “Secure federated submodel learning,” *arXiv preprint arXiv:1911.02254*, 2019.
- [26] C. Xie, S. Koyejo, and I. Gupta, “Practical distributed learning: Secure machine learning with communication-efficient local updates,” *arXiv preprint arXiv:1903.06996*, 2019.
- [27] T. Li, M. Sanjabi, and V. Smith, “Fair resource allocation in federated learning,” *arXiv preprint arXiv:1905.10497*, 2019.
- [28] S. Wang, T. Tuor, T. Salonidis, K. K. Leung, C. Makaya, T. He, and K. Chan, “Adaptive federated learning in resource constrained edge computing systems,” *IEEE J. Select. Areas Commun.*, vol. 37, no. 6, pp. 1205–1221, 2019.
- [29] D. Alistarh, D. Grubic, J. Li, R. Tomioka, and M. Vojnovic, “QSGD: Communication-efficient SGD via gradient quantization and encoding,” in *Advances in Neural Information Processing Systems*, 2017, pp. 1709–1720.
- [30] G. Zhu, Y. Du, D. Gunduz, and K. Huang, “One-bit over-the-air aggregation for communication-efficient federated edge learning: Design and convergence analysis,” *arXiv preprint arXiv:2001.05713*, 2020.
- [31] M. M. Amiri and D. Gündüz, “Federated learning over wireless fading channels,” *IEEE Trans. Wireless Commun.*, vol. 19, no. 5, pp. 3546–3557, 2020.
- [32] X. Mo and J. Xu, “Energy-efficient federated edge learning with joint communication and computation design,” *arXiv preprint arXiv:2003.00199*, 2020.
- [33] Z. Yang, M. Chen, W. Saad, C. S. Hong, and M. Shikh-Bahaei, “Energy efficient federated learning over wireless communication networks,” *arXiv preprint arXiv:1911.02417*, 2019.
- [34] H. H. Yang, Z. Liu, T. Q. Quek, and H. V. Poor, “Scheduling policies for federated learning in wireless networks,” *IEEE Trans. Commun.*, vol. 68, no. 1, pp. 317–333, 2020.
- [35] M. Chen, H. V. Poor, W. Saad, and S. Cui, “Convergence time optimization for federated learning over wireless networks,” *arXiv preprint arXiv:2001.07845*, 2020.
- [36] K. Yang, T. Jiang, Y. Shi, and Z. Ding, “Federated learning via over-the-air computation,” *IEEE Trans. Wireless Commun.*, vol. 19, no. 3, pp. 2022–2035, 2020.
- [37] Y. Sun, S. Zhou, and D. Gündüz, “Energy-aware analog aggregation for federated learning with redundant data,” in *IEEE International Conference on Communications (ICC)*, 2020, pp. 1–7.
- [38] —, “Energy-aware analog aggregation for federated learning with redundant data,” in *IEEE International Conference on Communications (ICC)*, 2020, pp. 1–7.
- [39] S. Caldas, J. Konečný, H. B. McMahan, and A. Talwalkar, “Expanding the reach of federated learning by reducing client resource requirements,” *arXiv preprint arXiv:1812.07210*, 2018.
- [40] F. Ang, L. Chen, N. Zhao, Y. Chen, W. Wang, and F. R. Yu, “Robust federated learning with noisy communication,” *IEEE Trans. Commun.*, vol. 68, no. 6, pp. 3452–3464, 2020.
- [41] P. Jiang and G. Agrawal, “A linear speedup analysis of distributed deep learning with sparse and quantized communication,” in *Advances in Neural Information Processing Systems*, 2018, pp. 2525–2536.
- [42] F. Zhou and G. Cong, “On the convergence properties of a k -step averaging stochastic gradient descent algorithm for nonconvex optimization,” in *Proc. IJCAI*, 2018, pp. 3219–3227.
- [43] H. Yu, R. Jin, and S. Yang, “On the linear speedup analysis of communication efficient momentum SGD for distributed non-convex optimization,” *arXiv preprint arXiv:1905.03817*, 2019.
- [44] S. Caldas *et al.*, “LEAF: A benchmark for federated settings,” *arXiv preprint arXiv:1812.01097*, 2018.